



Forecasting CPI inflation under economic policy and geopolitical uncertainties[☆]

Shovon Sengupta ^{a,b,1}, Tanujit Chakraborty ^{c,d,1,*}, Sunny Kumar Singh ^b

^a Fidelity Investments, Boston, USA

^b Department of Economics and Finance, BITS Pilani, Hyderabad, India

^c Department of Science and Engineering, Sorbonne University, Abu Dhabi, UAE

^d Sorbonne Center for Artificial Intelligence, Sorbonne University, Paris, France



ARTICLE INFO

Keywords:

Inflation forecasting

Wavelets

Neural networks

Empirical risk minimization

Conformal prediction intervals

ABSTRACT

Forecasting consumer price index (CPI) inflation is of paramount importance for both academics and policymakers at central banks. This study introduces the filtered ensemble wavelet neural network (FEWNet) to forecast CPI inflation, tested in BRIC countries. FEWNet decomposes inflation data into high- and low-frequency components using wavelet transforms, and incorporates additional economic factors, such as economic policy uncertainty and geopolitical risk, to enhance forecast accuracy. These wavelet-transformed series and filtered exogenous variables are input into downstream autoregressive neural networks, producing the final ensemble forecast. Theoretically, we demonstrate that FEWNet reduces empirical risk compared to fully connected autoregressive neural networks. Empirically, FEWNet outperforms other forecasting methods and effectively estimates prediction uncertainty, due to its ability to capture non-linearities and long-range dependencies through its adaptable architecture. Consequently, FEWNet emerges as a valuable tool for central banks to manage inflation and enhance monetary policy decisions.

© 2024 The Author(s). Published by Elsevier B.V. on behalf of International Institute of Forecasters. This is an open access article under the CC BY license (<http://creativecommons.org/licenses/by/4.0/>).

1. Introduction

The monetary policy framework at central banks relies heavily on forecasts of various macroeconomic variables. Forecasts have also grown in importance as a means of communication for central banks during the past 20 years, and they have the potential to shape public and market expectations. Numerous studies have examined central bank forecasting from various angles,

due to the paramount significance of these predictions (Faust & Wright, 2013; Nakamura, 2005; Pratap & Sengupta, 2019; Smalter Hall & Cook, 2017; Stock & Watson, 2007). Forecasting, particularly in the context of different macroeconomic policy variables, is one of the major focus areas in this domain. Inflation is one such policy variable considered instrumental in designing an economy's overall monetary policy. Thus, a deeper understanding of the factors that help forecast inflation accurately is fundamental to policymakers at the central bank (Stock & Watson, 2007). Over the past few decades, emerging market economies such as Brazil, Russia, India, and China (BRIC) have undergone significant changes in their macroeconomic conditions, including shifts in monetary policy frameworks such as inflation targeting, increased globalization, and the impact of events like the financial crisis and the recent pandemic. These shifts

[☆] The numerical results presented in the paper were reproduced by the Editor-in-Chief on 10 September 2024.

* Corresponding author.

E-mail addresses: shovon.sengupta@fmr.com (S. Sengupta), tanujit.chakraborty@sorbonne.ae (T. Chakraborty), sunny.singh@hyderabad.bits-pilani.ac.in (S.K. Singh).

¹ S. Sengupta and T. Chakraborty are joint first authors.

make predicting key macroeconomic variables like consumer price index (CPI) inflation quite challenging (Pratap & Sengupta, 2019). Given these dynamic changes in the macroeconomic environment, factors like economic policy uncertainty and geopolitical risk might offer critical insights to forecast inflation accurately.

Given the critical importance of inflation forecasting for monetary policy, central banks frequently rely on both structural and non-structural models. Structural models, often various iterations of Phillips curve models, are rooted in economic theory. In contrast, non-structural models, including univariate and multivariate time series models, leverage the intrinsic characteristics of the data without relying on explicit economic theory (Faust & Wright, 2013). These non-structural models prioritize forecast accuracy over causal inference, making them particularly valuable for short-term, out-of-sample forecasting. However, traditional linear time series models, such as the autoregressive integrated moving average (ARIMA) and vector autoregressive (VAR) models, face limitations in capturing business cycles, periods of extreme volatility induced by macroeconomic uncertainties, and structural changes. Consequently, non-linear, hybrid, and machine learning models have gained prominence in overcoming these limitations (Chakraborty, Chakraborty, Biswas, Banerjee, & Bhattacharya, 2021; Panja, Chakraborty, Kumar & Liu, 2023; Sasal, Chakraborty, & Hadid, 2022). Additionally, existing linear time series forecasting methods exhibit undesirable properties, such as high sensitivity to model specification and a need for high-frequency data (Smalter Hall & Cook, 2017). These challenges are particularly significant when forecasting inflation or other macroeconomic variables that are available only at monthly, quarterly, or annual frequencies. Machine learning models and combined approaches offer a promising avenue for enhancing the forecast performance of inflation data in emerging economies.

Recently, there has been a surge in studies exploring the application of machine learning (ML) models for inflation forecasting in both advanced and emerging market economies. For instance, a study in the United States employed a basic feed-forward neural network to forecast quarterly CPI inflation, demonstrating its effectiveness at prediction (Nakamura, 2005). Neural networks have also shown superior performance in forecasting monthly inflation rates for OECD countries, outperforming traditional models in 45% of the cases compared to 23% for simple AR models (Choudhary & Haider, 2012). Various forms of recurrent neural networks have been instrumental in predicting inflation in developed countries (Almosova & Andresen, 2023; Barkan, Benchimol, Caspi, Cohen, Hammer, & Koenigstein, 2023; Chen, Racine, & Swanson, 2001; McAdam & McNelis, 2005). Additionally, recent research has compared multiple ML models, including lasso regression, random forests, and deep neural networks, to analyze inflation in the United States, incorporating factors such as cash and credit availability, online prices, housing prices, consumer data, exchange rates, and interest rates. This study found that ML models with numerous covariates consistently outperformed traditional methods, attributed to their ability to capture non-linear

relationships between historical macroeconomic variables and inflation (Medeiros, Vasconcelos, Veiga, & Zilberman, 2021). This evidence dispels skepticism about using ML and modern deep learning architectures in economic data analysis (Mullainathan & Spiess, 2017). In emerging market economies, the application of advanced ML models for inflation forecasting remains in its early stages. Neural network applications are noted in developing countries such as India, Brazil (Araujo & Gaglianone, 2023), Russia (Pavlov, 2020), Turkey, South Africa (Botha, Burger, Kotzé, Rankin, & Steenkamp, 2023), and China (Özgür & Akkoç, 2021). However, to the best of our knowledge, none of these studies have incorporated exogenous factors like macroeconomic uncertainties for inflation forecasting, particularly in emerging markets.

Following events such as the global financial crisis, many countries worldwide have encountered heightened uncertainty, significantly impacting decision-making processes and the overall macroeconomy (Baker, Bloom, & Davis, 2016; Bloom, 2009, 2014). While previous studies have primarily examined the connection between uncertainty and the macroeconomy, the evaluation of the evolving relationship between measures of uncertainty and inflation remains in its nascent stages (Jones & Olson, 2013; Leduc & Liu, 2016). Understanding the intricacies of inflation dynamics and uncertainty metrics is crucial for policymakers. Recent studies indicate that both economic policy uncertainty (EPU) and geopolitical risk (GPRC) significantly influence inflation dynamics (Adeosun, Tabash, Vo, & Anagreh, 2023; Anderl & Caporale, 2023; Balcilar, Gupta, & Jooste, 2017; Benchimol & El-Shagi, 2020; Caldara & Iacoviello, 2022; Colombo, 2013; Jones & Olson, 2013). Therefore, failure to incorporate these uncertainties may result in incorrect specifications of inflation forecasting models. Balcilar et al. (2017) investigated the effectiveness of different uncertainty measures in predicting inflation, using U.S. inflation data and the EPU index to compare the performance of the vector autoregressive fractionally integrated moving average (VAFIMA) model against other models. Salisu, Demirer, and Gupta (2023) examined the predictive impact of EPU on stock market volatility in the United States and the United Kingdom, finding a significant positive effect that weakens with low signal quality. Liu and Zhang (2015) asserted that EPU enhances the predictive accuracy of models forecasting stock market volatility. Jones and Sackley (2016) investigated the impact of policy uncertainty on the short-term pricing model for gold in the United States and Europe. Junttila and Vataja (2018) examined the impact of EPU on predicting future real economic activities in the UK and European economies. Al-Thaqeb and Algharabali (2019) provided an extensive analysis of methods for quantifying uncertainty and its impact on various economic activities, such as stock market returns, corporate capital investments, and risk management. Caldara and Iacoviello (2022) extensively studied the effects of geopolitical risk (GPRC), while (Pringpong, Maneenop, & Jaroenjitrkam, 2023) linked geopolitical risk with the reduction of firm values. This study aimed to accommodate the roles of EPU and GPRC in forecasting inflation, addressing a critical gap in the literature on the impact of various uncertainty measures on economic activities.

Wavelet analysis has shown remarkable promise for analyzing financial time series, due to its ability to distillate crucial information from the data. Its structural flexibility allows it to handle irregular time series data more effectively for long-term time series forecasting (Percival & Guttorm, 1994). Broadly, wavelets decompose the original time series into two sub-components: one concerning the low-frequency or deterministic component, and the other concerning the high-frequency or stochastic component of the series. This process aims to reduce the effect of 'noise' in the forecast and is found to be quite useful for dealing with a variety of non-stationary signals, a common feature of financial and macroeconomic time series data, as they are constructed over finite time intervals and can represent the 'local' elements in both time and scale (Percival & Walden, 2000). Several applications of wavelet analysis can be found in forecasting exchange rates, GDP growth, crude oil prices, stock market prices, the Taiwan stock index, S&P dividend yield, trade prices, expenditure and income, price movements, money growth, inflation (Shrestha & Tan, 2005; Yousefi, Weinreich, & Reinartz, 2005), volatility in foreign exchange markets, and car sales from the last decades (Crowley, 2007). A wide variety of hybrid models combining wavelets and neural networks have been studied for forecasting natural gas prices (Jin & Kim, 2015), futures trading (Zhang, Coggins, Jabri, Dersch, & Flower, 2001), short-term electricity load (Benaouda, Murtagh, Starck, & Renaud, 2006; Zhang & Dong, 2001), energy price forecasting (Tan, Zhang, Wang, & Xu, 2010), oil prices (Yousefi et al., 2005), and stock indices (Dunis & Williams, 2002). Several studies have employed wavelet-based forecasting methods in various other domains of economics, business, and finance. For instance, Fernandez (2007) focused on the U.S. metal and materials manufacturing industry, employing wavelet decomposition combined with support vector machines to enhance forecasting accuracy. While the study effectively captured complex dynamics in manufacturing, it did not address long-term forecasting horizons or the inclusion of exogenous variables, which are crucial for economic forecasting. Rua (2017) used wavelet-based multiscale principal component analysis to improve factor model estimation and forecasting of macroeconomic variables like GDP growth and inflation in the U.S. Another paper by Souropanis and Vivian (2023) enhanced realized volatility forecasts for the S&P 500 using wavelet decomposition coupled with an autoregressive model. However, these approaches do not address the non-linearity issue, as evident in CPI inflation data. In recent work, He, Gong, and Huang (2021) used a deep learning framework enhanced by wavelet transform to predict multivariate time series. Although their model captures the long-term and short-term characteristics of time series in the temporal domain through convolutional neural networks, it cannot be generalized well for limited inflation time series data problems. Vogl, Rötzel, and Homes (2022) utilized the efficacy of combining wavelet functions with neural networks for financial market predictions. More recently, Boubaker, Canarella, Gupta, and Miller (2023) proposed a hybrid model based on ARFIMA and a wavelet neural network for forecasting

the DJIA index. However, the exclusion of exogenous variables and focus on high-frequency data limits its applicability to macroeconomic forecasting of CPI inflation. Apart from forecasting applications, wavelet analysis has been used in various areas of finance: (Kim & In, 2005) analyzed the association between stock price and inflation rate using wavelet analysis, Rua and Nunes (2012) explored the aspect of assessing risk in emerging markets, and He, Lai, and Yen (2012) studied the value at risk in metal markets. Alexandridis and Hasan (2020) examined the impact of the global financial crisis on the multi-horizon nature of systematic risk and market risk using a wavelet multi-scale approach. Becerra, Galvão, and Abou-Seada (2005) used wavelet neural networks for the prediction of corporate financial distress. However, none of the above studies have utilized the inflation series and its causal counterparts for long-term forecasting.

Our study aimed to develop a filtered ensemble wavelet neural network (FEWNet) model for CPI inflation forecasting, focusing on generating accurate long-term forecasts for BRIC countries while considering economic policy uncertainty (EPU) and geopolitical risk composite (GPRC) indices. FEWNet's robustness in handling non-linear, non-stationary, and complex time series is demonstrated through its superior performance against a range of baseline models, from classical time series to modern deep learning architectures. Macroeconomic policy variables, characterized by low-frequency data, often pose challenges for models effective with high-frequency data. To extract low-frequency components without compromising the fundamental characteristics of the original time series, we employ wavelet decomposition in this context. The model integrates feature engineering using the Hodrick–Prescott (HP) filter for trend components and the Christiano–Fitzgerald (CF) ideal band-pass filter for cyclical elements. Initially, we decompose the observed time series (CPI inflation) and exogenous factors (EPU and GPRC) into their trend and cyclical components using HP and CF filters. In the second phase, these components, along with wavelet-transformed details and smooth coefficients of CPI inflation, are modeled as auxiliary inputs within the FEWNet framework. This comprehensive approach aims to generate 12- and 24-month-ahead forecasts, capturing the inflationary or deflationary effects of uncertainty through wavelet coherence analysis, which indicates a relationship between EPU, GPRC, and CPI inflation for BRIC economies. FEWNet generates out-of-sample forecasts recursively and is evaluated using several statistical metrics and tests, comparing its performance with alternative forecasting methods. Theoretical results on empirical risk minimization are presented to support FEWNet's efficacy. The study assesses various neural network architectures and statistical benchmarks, demonstrating that FEWNet delivers superior forecasting performance for both semi-long-term (12 months ahead) and long-term (24 months ahead) horizons for CPI inflation series in BRIC countries. Beyond improved forecast accuracy, understanding how structural uncertainties influence the dynamic behavior of macroeconomic variables is crucial for policymakers. FEWNet's performance surpasses its counterparts in all BRIC economies, except

China, illustrating its effectiveness at managing complex, non-stationary time series for forecasting tasks.

The paper is organized in the following way. Section 2 explains the macroeconomic series considered in this study, various data pre-processing strategies, and the causal association between the uncertainty indices and CPI inflation. Section 3 focuses on the proposed methodology with a detailed overview of its architectural design, and Section 4 theoretically establishes the robustness of the method from an empirical risk minimization perspective. Section 5 discusses the experimental evaluation and the process of deriving a conformal prediction interval for the FEWNet framework. We discuss policy implications in Section 6. Finally, Section 7 wraps up the study by presenting a thorough analysis of the main discoveries and outlining potential future directions.

2. Data and preliminary analysis

This work is premised on forecasting the monthly CPI inflation series for four countries—Brazil, Russia, India, and China—based on their historical data and various economic uncertainty measures such as EPU and GPRC. To evaluate the performance of our proposed method, we consider two forecast horizons, namely, a semi-long-term length of 12 months and a long-term length of 24 months, for each of the countries. This section details the datasets used in our analysis, their properties, the steps involved in data preparation (Section 2.1), and the causality analyses conducted (Section 2.2).

2.1. Data preparation and global characteristics

In this study, we use monthly data on CPI inflation, EPU, and GPRC for BRIC countries from January 2003 (2003–01) to November 2021 (2021–11). For the semi-long-term forecasting task, we set the training period from 2003–01 to 2020–11 and the test horizon as 2020–12 to 2021–11. For long-term forecasting, our training data span from 2003–01 to 2019–11 and the test period extends from 2019–12 to 2021–11. Our target CPI inflation (also headline inflation) is measured as the year-on-year percentage change in the consumer price index (CPI) series obtained from Federal Reserve Economic Data (FRED) (<https://fred.stlouisfed.org/>). These numbers are seasonally unadjusted and are calculated based on the following approach:

$$\pi_{\text{Jan}}^{2003} = \left[\frac{\text{CPI}_{\text{Jan}}^{2003} - \text{CPI}_{\text{Jan}}^{2002}}{\text{CPI}_{\text{Jan}}^{2002}} \right] * 100\%, \quad (1)$$

where π_{Jan}^{2003} denotes the derived CPI inflation number for 2003-Jan, calculated using CPI values of January, 2003, and January, 2002 (prior year and same month).

We use two of the most popular news-based measures of uncertainty: the EPU index developed by Baker et al. (2016), and the GPRC index developed by Caldara and Iacoviello (2022). EPU represents the likelihood of changes in monetary, fiscal, or regulatory policies that can impact the decision-making behavior of investors and consumers (Baker et al., 2016). According to Baker et al. (2016), the EPU index is constructed by analyzing the

frequency of certain terms in newspaper articles from a variety of sources, including the Access World News Bank Service. The index captures articles that mention key terms related to economic and policy uncertainty. Specifically, it searches for combinations of terms such as 'economics', 'deficit', 'uncertainty', 'monetary policy', 'regulation', 'legislation', 'White House', 'Federal Reserve', or 'Congress'. This electronic text search process helps quantify the level of policy uncertainty by tracking the presence of these terms over time in major newspapers. The data on EPU are sourced from <http://www.policyuncertainty.com/>. Similarly, the GPRC index measures the occurrence of geopolitical events such as terrorism, local and regional political instability, political violence, coups, territorial conflicts, and war. These events contribute to the uncertainty in the geopolitical landscape. According to Caldara and Iacoviello (2022), the GPRC index is constructed by conducting electronic text searches of specific terms related to geopolitical tensions across 10 prominent daily newspapers. The GPRC index categorizes search terms into eight distinct categories to measure various facets of war-related events and geopolitical tensions: War Threats (1), Peace Threats (2), Military Buildups (3), Nuclear Threats (4), Terror Threats (5), Beginning of War (6), Escalation of War (7), and Terror Acts (8). Data on GPRC are obtained from <https://www.matteoiacoviello.com/gpr.htm>.

As part of the data pre-processing step, we perform a log transformation on the EPU series to stabilize its variance. Sequentially, we decompose the CPI inflation, log-transformed EPU, and GPRC series using the Hodrick and Prescott (HP) filter (Hodrick & Prescott, 1997) and the Christiano–Fitzgerald (CF) random walk filter (Christiano & Fitzgerald, 2003). These economic filters play a vital role in extracting the trends and business cycles associated with the time series. Further details on the HP filter and CF filter are provided in Appendix A.3. Summary statistics of the variables under study are provided in Table 1.

In the analysis, we study the global features of the CPI inflation series, log-transformed EPU series, and GPRC series to identify their structural patterns and detect appropriate techniques for long-term forecasting. Primarily, we focus on seven popular time series characteristics: skewness, kurtosis, non-linearity, long-range dependence, seasonality, stationarity, and outlier check (Hyndman & Athanasopoulos, 2018). We utilize the Hurst exponent to assess the long-range dependency of the time series. To analyze the non-linear characteristics of the series, we employ Tsay's test and Keenan's one-degree test for non-linearity. To determine the stationarity of the series, we conduct the Kwiatkowski–Phillips–Schmidt–Shin test. Lastly, we apply Ollech and Webel's test to identify any seasonal patterns in the series. The results of the statistical features, summarized in Table 2, show that most of the macroeconomic time series are non-stationary, except for the GPRC series of Brazil and the CPI inflation data of China. The majority of these series are positively skewed, except for the log-transformed EPU series of Russia. Furthermore, most of the economic time series exhibit non-linear patterns, which play a crucial role in selecting the appropriate modeling approach for the dataset. Additionally, based on Ollech and Webel's seasonality test

Table 1

Summary statistics of the datasets used in this study.

Countries	Series	Obs.	Min. value	Max. value	Q_1	Median	Mean	Q_3	CoV	Entropy
Brazil	CPI Inflation	227	1.88	17.24	4.31	5.7	6.11	6.86	46.86	5.41
	log(EPU)	227	1.35	2.83	2.00	2.15	2.16	2.3	10.94	5.65
	GRPC	227	0.01	0.23	0.03	0.04	0.05	0.06	66.08	15.13
Russia	CPI Inflation	227	2.2	16.93	5.46	7.61	8.44	11.60	46.01	5.38
	log(EPU)	227	1.38	2.90	1.96	2.15	2.15	2.35	13.28	5.65
	GRPC	227	0.22	2.23	0.42	0.58	0.67	0.83	51.46	6.05
India	CPI Inflation	227	1.08	16.22	4.51	6.09	6.69	8.70	43.43	5.41
	log(EPU)	227	1.37	2.45	1.72	1.90	1.90	2.06	11.70	5.68
	GRPC	227	0.06	0.89	0.14	0.18	0.20	0.24	44.93	7.86
China	CPI Inflation	227	-1.79	8.81	1.51	2.11	2.52	3.21	75.55	5.47
	log(EPU)	227	1.42	2.99	1.96	2.18	2.24	2.51	16.97	5.63
	GRPC	227	0.21	1.52	0.36	0.47	0.53	0.65	46.05	6.27

Table 2

Global characteristics of the economic time series under study for BRIC countries.

Countries	Series	Skewness	Kurtosis	Non-linearity	Long-range dependence	Seasonality	Stationarity	Outlier
Brazil	CPI Inflation	1.67	3.57	Non-linear	0.73	Non-seasonal	Non-stationary	No outliers detected
	log(EPU)	-0.9	0.29	Non-linear	0.77	Non-seasonal	Non-stationary	1 outlier detected
	GRPC	2.06	6.60	Non-linear	0.63	Non-seasonal	Stationary	4 outliers detected
Russia	CPI Inflation	0.28	-0.98	Linear	0.78	Non-seasonal	Non-stationary	No outliers detected
	log(EPU)	-0.03	-0.12	Non-linear	0.79	Non-seasonal	Non-stationary	No outliers detected
	GRPC	1.41	2.46	Linear	0.79	Non-seasonal	Non-stationary	2 outliers detected
India	CPI Inflation	0.71	0.17	Linear	0.82	Non-seasonal	Non-stationary	No outliers detected
	log(EPU)	0.12	-0.47	Linear	0.80	Non-seasonal	Non-stationary	No outliers detected
	GRPC	2.51	15.22	Non-linear	0.73	Non-seasonal	Non-stationary	1 outlier detected
China	CPI Inflation	0.82	1.08	Non-linear	0.69	Non seasonal	Stationary	No outliers detected
	log(EPU)	0.23	-0.87	Non-linear	0.82	Non-seasonal	Non-stationary	No outliers detected
	GRPC	1.28	1.51	Non-linear	0.80	Non-seasonal	Non-stationary	1 outlier detected

and the Hurst exponent, we observe that all the series are non-seasonal and are characterized by long-range dependency. Moreover, the ACF and PACF plots of the CPI inflation series (presented in Table 3) depict the presence of serial autocorrelation. These inherent patterns of the CPI inflation series motivate the design and application of hybrid forecasting approaches for long-term forecasting. We also performed the Bonferroni outlier test (Weisberg & Cook, 1982) based on Studentized residuals. Our findings indicate that none of the CPI inflation series have significant outliers based on the adjusted p-values. However, while inflation remains relatively steady, policy uncertainty and geopolitical risks experience sudden and substantial fluctuations. This differential behavior underscores the need for policymakers to vigilantly monitor these indicators and implement strategic interventions aimed at mitigating the adverse effects of such outliers on the broader economy. We further examined the presence of structural breakpoints in the CPI inflation series to account for regime shifts and their potential impact on our downstream forecasting models, utilizing the ordinary least squares (OLS)-based CUSUM test (Ploberger & Krämer, 1992). By examining the cumulative sum of recursive residuals, the test can reveal deviations from the model's stability, indicating potential breakpoints. In our study, the application of the OLS-based CUSUM test allows us to isolate and identify periods of structural change in the CPI inflation series. The CPI inflation series for these countries does not exhibit statistically significant breakpoints. The absence of statistically significant breakpoints

in the CPI inflation series for Brazil, Russia, India, and China suggests that these series have remained relatively stable over the observed period. This stability implies that regime shifts are unlikely to pose significant challenges for forecasting models based on these series.

2.2. Causality analysis

This section explores the causal impact of log-transformed EPU and GPRC uncertainties on the CPI inflation series for BRIC countries. Several statistical methods, such as the Granger causality test, cross-convergent mappings, and transfer entropy, have been suggested in the literature to examine the causal relationship between two variables (Pierce & Haugh, 1977). Nevertheless, the tests rely on certain data-level assumptions that are not met in the macroeconomic series analyzed in this work. In order to address this constraint, we employ wavelet coherence analysis (WCA) to examine the causal relationship between the series (Grinsted, Moore, & Jevrejeva, 2004). WCA is a valuable method for examining the interconnection and simultaneous movement of two non-stationary signals in the time-frequency domain.

In the WCA plots, shown in Fig. 1, the first row depicts the WCA results between CPI inflation and log-transformed EPU series, and the second row shows the same for CPI inflation and GPRC series. In each of the plots, the horizontal axis measures the time, and the vertical axis shows the frequency dimension. Wavelet coherence represents the regions in the time-frequency

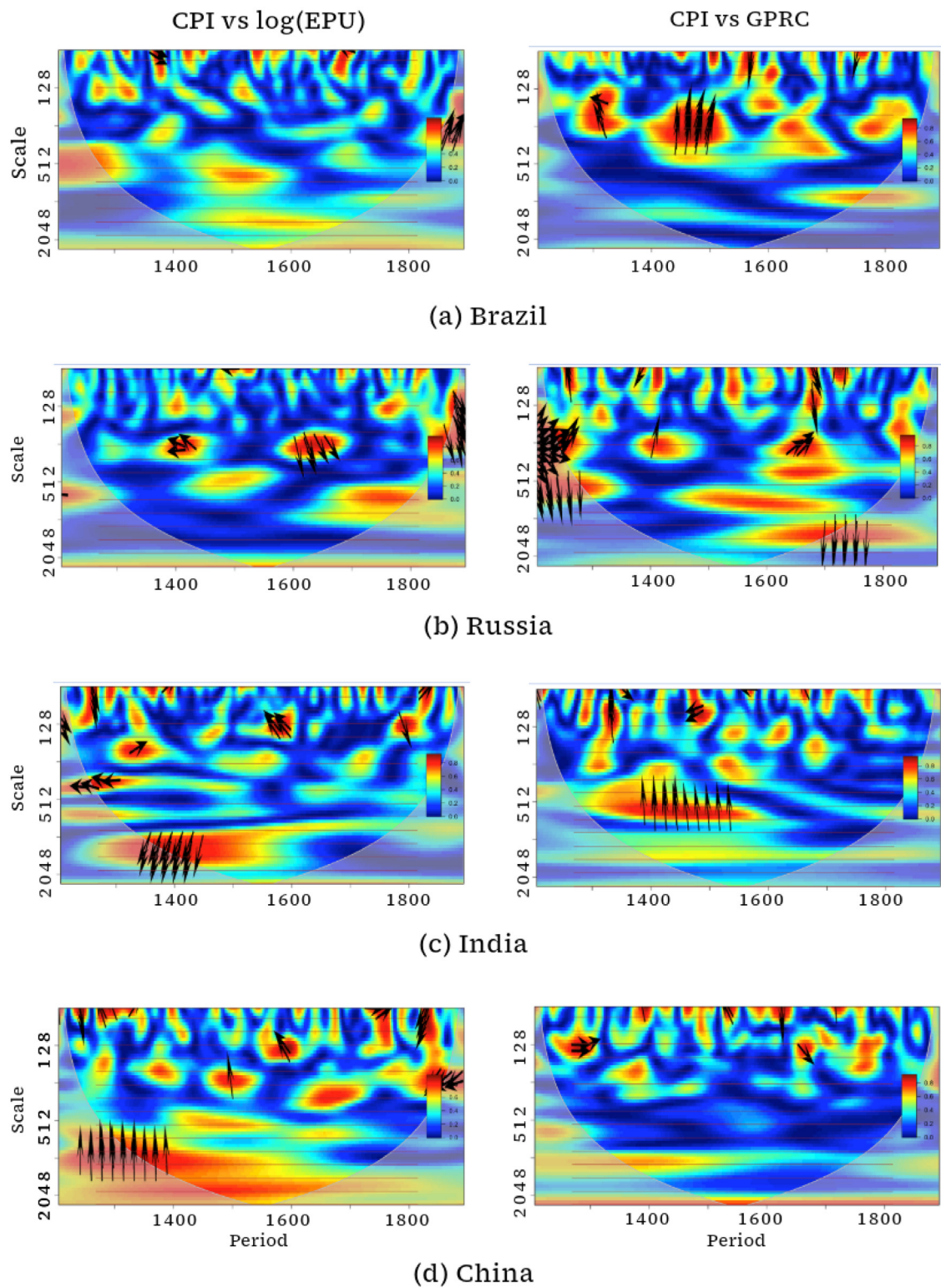
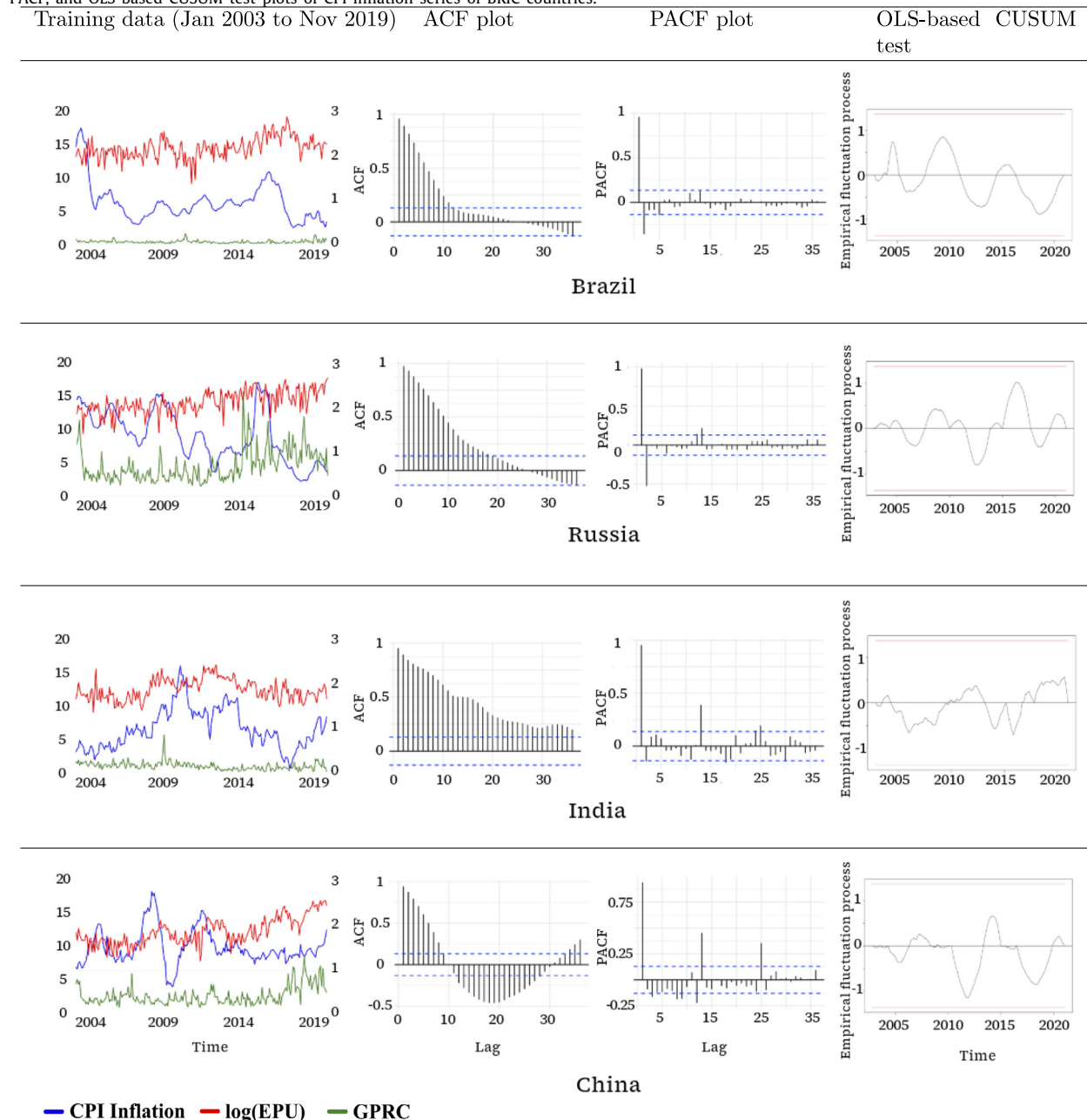


Fig. 1. Wavelet coherence analysis plots of CPI inflation with log-transformed EPU (left) and CPI inflation with GPRC (right) for (a) Brazil, (b) Russia, (c) India, and (d) China.

Table 3

Training data for FEWNet, including target-series CPI inflation (blue) and the exogenous variables log-transformed EPU (red) and GPRC (green). ACF, PACF, and OLS-based CUSUM test plots of CPI inflation series of BRIC countries.



domain where the two signals co-vary. In the plot, the transition from warmer colors (red) to colder colors (blue) respectively indicates regions from higher coherence to lower coherence between the series. The arrow in the WCA plots indicates the lag phase relations between the analyzed signals. A zero-phase difference would hint toward the co-movement of the signals on any particular scale. The direction of an arrow has a specific connotation, with the arrows pointing to the right (left) indicating that the signals are in phase (anti-phase), i.e., the two signals are moving in the same direction, or vice versa. As evident

from the plots, there exists a significant causal relation between CPI inflation, log-transformed EPU, and GPRC series. This, in turn, justifies the choice of EPU and GPRC as exogenous factors in forecasting the CPI inflation series of BRIC countries.

3. Proposed FEWNet model

This section provides a comprehensive description of our proposed architecture, called the filtered ensemble wavelet neural network (FEWNet). FEWNet combines the

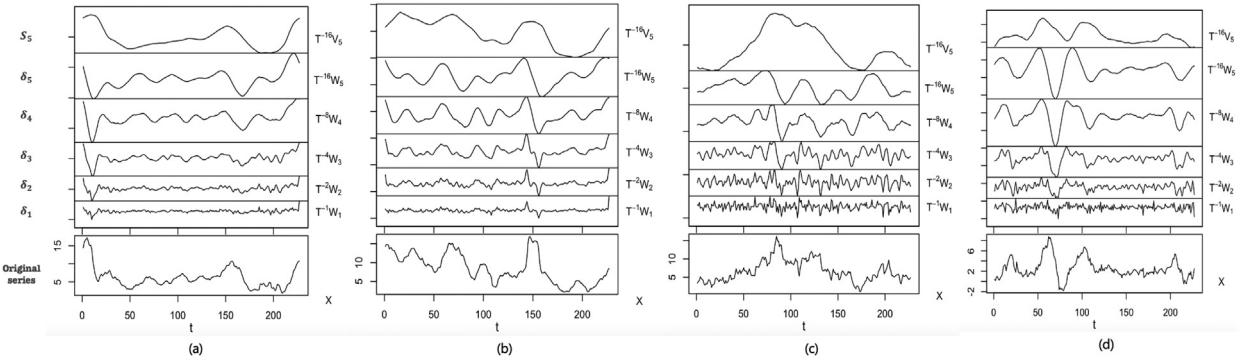


Fig. 2. MODWT decomposition of the CPI inflation series for (a) Brazil, (b) Russia, (c) India, and (d) China from January 2003 to November 2021. In these figures, $\delta_1, \delta_2, \dots, \delta_5$ and S_5 represent the details and smooth of the series generated by the MODWT-based MRA approach. The bottom chart in all the figures represents the original time series (CPI inflation) in actual frequency scale.

maximal overlapping discrete wavelet transformation (MODWT) technique (explained in [Appendix A.1](#)), economic filtering methods such as the Hodrick–Prescott (HP) filter and Christiano–Fitzgerald (CF) filter (explained in [Appendix A.3](#)), and an autoregressive neural network with exogenous variables (ARNNx). The FEWNNet framework is a sequential approach that initially decomposes the CPI inflation data into low-frequency (smooth) and \mathcal{K} high-frequency (detail) components using the scaling and wavelet filters of MODWT, as depicted in [Fig. 2](#). The ability of the transition and time-invariant MODWT approach to handle the non-stationary features of the time-dependent signal makes it a valuable tool for pre-processing the CPI inflation dataset. Simultaneously, to capture the economic uncertainties of the time series, we apply the CF and HP filters on the CPI, log-transformed EPU, and GPRC series. The non-parametric CF filter efficiently captures the trend components, whereas the HP filter is suitable for identifying and modeling the business cycles. This long-term trend and the repetitive cyclical patterns were found to provide significant information regarding the economic uncertainties that impact the future trajectories of the CPI inflation series.

The real-world CPI inflation series exhibit notable features, including non-stationarity, non-linearity, and long-term dependence, as evidenced in [Table 2](#). In order to accurately represent this non-uniform time series, we utilize MODWT decomposition using Daubechies orthogonal wavelets of length 2, namely the Haar filter. This transformation has the ability to identify the specific time and frequency components of signals, successfully distinguishing between long-range connections, non-stationarity, and patterns within the signals ([Percival & Mofjeld, 1997](#)). By utilizing MODWT-based multi-resolution analysis (MRA) decomposition on the series Y_t , we derive a collection of $\mathcal{K} + 1$ distinct random variables called wavelet and scaling coefficients, which are not correlated with each other. In our suggested methodology, we employ separate neural networks within an ensemble framework to represent $\mathcal{K} + 1$ random variables instead of employing the original CPI inflation series Y_t . These neural networks are specifically engineered and trained to effectively manage the intricacies linked to the wavelet coefficients. By employing this approach, we may efficiently tackle the non-linear nature

observed in the CPI inflation data of BRIC nations. In addition, in order to capture the temporal causal association between the input series and the exogenous variables ($X_{j,t}, j = 1, 2, \dots, 6$), we include them in each of the $\mathcal{K} + 1$ wavelet transformed series of Y_t in their corresponding neural networks. The forecasts produced by these $\mathcal{K} + 1$ neural networks are combined to determine the future dynamics of Y_t . The mathematical expression for the m -step-ahead forecasts of Y_t , designated as $\hat{Y}_{\mathcal{N}+m}$ based on \mathcal{N} past data, is as follows:

$$\hat{Y}_{\mathcal{N}+m} = \hat{S}_{\mathcal{K}, \mathcal{N}+m} + \sum_{\tilde{k}=1}^{\mathcal{K}} \hat{\delta}_{\tilde{k}, \mathcal{N}+m}, \quad (2)$$

where $\hat{S}_{\mathcal{K}, \mathcal{N}+m}$ and $\hat{\delta}_{\tilde{k}, \mathcal{N}+m}$, $\tilde{k} = 1, 2, \dots, \mathcal{K}$ are the forecasts generated from the simultaneously computed neural networks of the smooth series $S_{\mathcal{K}, t}$ and the details series $\delta_{\tilde{k}, t}$, $\tilde{k} = 1, 2, \dots, \mathcal{K}$. Each of these $\mathcal{K} + 1$ neural networks consists of a feedforward design with three layers: the input layer with p nodes, one hidden layer with q nodes, and one output layer without any shortcut connections. The neural networks model incorporates $p - 6$ lagged observations of the wavelet coefficients, as well as one lagged observation for each of the six exogenous variables (X_j). These variables represent the trend and cycle information of CPI, log-transformed EPU, and GPRC. This setting allows the networks to generate one-step-forward forecasts for the related series. Mathematically, the result obtained from each neural network after one iteration can be represented as follows:

$$\begin{aligned} \hat{\delta}_{\tilde{k}, \mathcal{N}+1} &= \alpha_{0, \tilde{k}} + \sum_{i=1}^q \beta_{i, \tilde{k}} \sigma(\alpha_{i, \tilde{k}} + \beta'_{i, \tilde{k}} \vec{\delta}_k + \gamma'_{i, \tilde{k}} \underline{X}); \quad \tilde{k} = 1, 2, \dots, \mathcal{K} \\ \hat{S}_{\mathcal{K}, \mathcal{N}+1} &= \alpha_0^S + \sum_{i=1}^q \beta_i^S \sigma(\alpha_i^S + \beta_i^{S'} \vec{S}_{\mathcal{K}} + \gamma_i^{S'} \underline{X}), \end{aligned} \quad (3)$$

where $\vec{\delta}_k$ and $\vec{S}_{\mathcal{K}}$ denote the $p - 6$ lagged observation of the corresponding wavelet coefficients; \underline{X} indicates a single lagged vector of exogenous variables; $\alpha_{0, \tilde{k}}, \alpha_0^S, \alpha_{i, \tilde{k}}, \alpha_i^S$, and β_i are the bias terms; $\beta_{i, \tilde{k}}$ and β_i^S are the connection weights between the hidden and output layers; $\gamma'_{i, \tilde{k}}$ and $\gamma_i^{S'}$ are

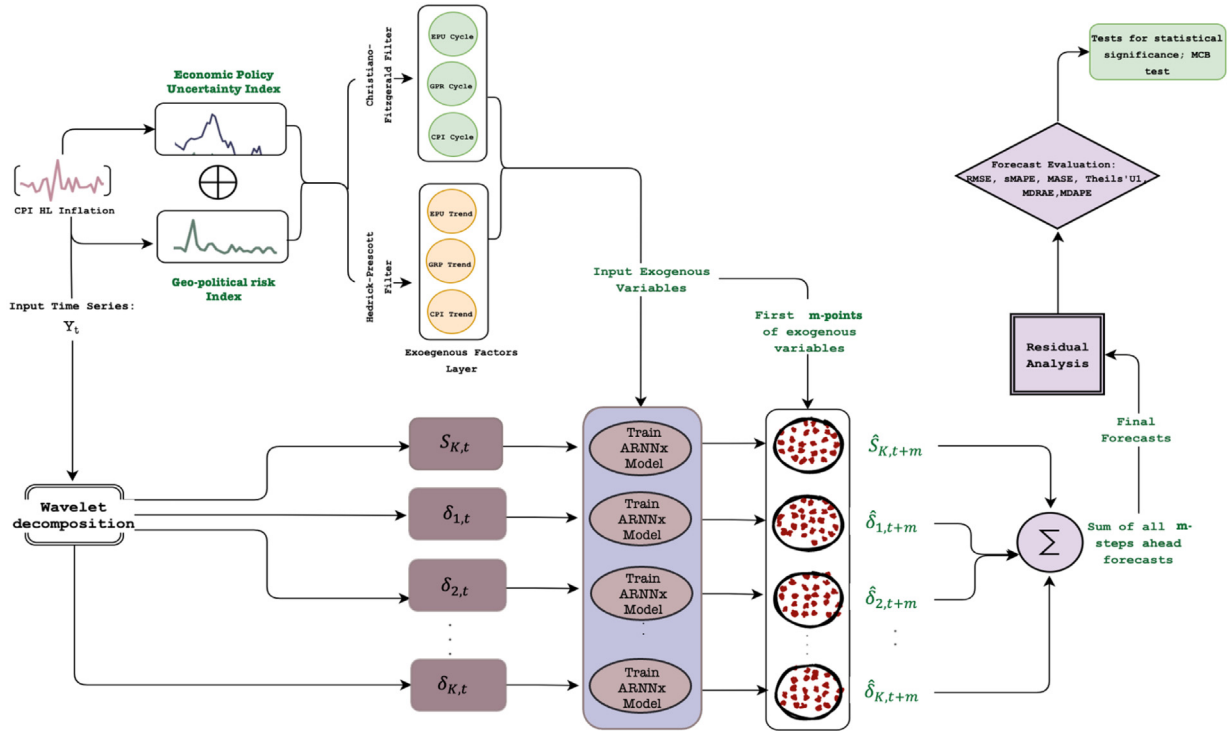


Fig. 3. Illustration of the proposed FEWNet model.

the weight vectors between the exogenous variables and the hidden layer; $\beta'_{i,\bar{k}}$ and $\beta^{S'}_i$ are the connection weights between lagged wavelet series and the hidden layer; and σ indicates the non-linear activation function.

Within our framework, we commence by assigning random initial values to the connection weights. Subsequently, we employ the gradient descent back-propagation approach to train these weights, as described in the work by Rumelhart, Hinton, and Williams (1986). The aforementioned technique produces a forecast that is one step ahead for each of the wavelets and scaling coefficients. In order to make forecasts for several future time steps, we incorporate the most recent predictions into the input layer instead of using the last observed value, and we continue this procedure recursively. Ultimately, we combine the predictions produced by each of the base models in an ensemble setup and derive the forecast for a desired time horizon.

The FEWNet algorithm consists of three hyperparameters: the level of MODWT decomposition (K), the number of lagged observations in the input layer (p), and the number of hidden nodes (q). Prior research has indicated that selecting the appropriate level of wavelet decomposition (K) is vital for distinguishing the genuine signal from noise in a complicated series (Aussem & Murtagh, 1997; Percival & Mofjeld, 1997). In order to limit the computational cost of the shift-invariant MODWT technique, we choose $K = \lfloor \log_e(\text{length of training set}) \rfloor = \lfloor \log_e N \rfloor$, where $\lfloor \cdot \rfloor$ denotes the floor function, following (Percival & Walden, 2000). To specify the number of previous lagged observations in the input layer, we utilize the

cross-validation strategy and select p so that it minimizes the symmetric mean absolute percent error (SMAPE) of the validation set:

$$p = \underset{p}{\operatorname{argmin}} \frac{1}{|\mathcal{V}|} \sum_{t \in \mathcal{V}} \frac{2|\hat{Y}_t - Y_t|}{|\hat{Y}_t| + |Y_t|}, \quad (4)$$

where \mathcal{V} indicates the validation set, and Y_t and \hat{Y}_t are the original series and forecast at time t , respectively. Moreover, to stabilize the learning rate of the neural network, restrict overfitting, and reduce the run-time of the proposed FEWNet framework, we set the number of hidden nodes arranged in a single hidden layer as $q = \lceil \frac{p+1}{2} \rceil$ (rounded to the nearest integer) following (Panja, Chakraborty, Kumar et al., 2023). The proposed FEWNet model is illustrated in Fig. 3 using a schematic approach. The target time series is initially subjected to an MODWT-based MRA, resulting in multiple degrees of transformation, as shown in the figure. The economic uncertainties and geopolitical risk index series are filtered along with the CPI inflation series using the CF filter and HP filter to generate the corresponding cycle (green circles) and trend (yellow circles), respectively. These six exogenous variables are then provided with the lagged wavelet series in the input layer of each of the $K + 1$ neural networks. The connection weights establish the connections between each input set and the hidden nodes, represented as lines with arrows. The results from the hidden layer are processed in the output layer, ultimately producing the forecast for the next step from the interconnected network. Ultimately, the future dynamics of the CPI inflation series are formed by producing multi-step-ahead

forecasts in a recursive fashion and then combining them in an ensemble. The utilization of wavelet decomposition to reveal the complex variability of the transformed series and the subsequent modeling of these fluctuations with diverse economic filtered uncertainties using an autoregressive neural network with auxiliary information within an ensemble framework provide a valid rationale for naming the proposed model as FEWNet. The implementation methodology of the proposed FEWNet is outlined in Algorithm 1.

Remark 1. Conventional machine learning and deep learning frameworks, such as XGBoost and TFT, often use a sliding window approach to transform time series forecasting into a supervised learning task; our proposed FEWNet architecture takes a distinct approach. We utilize an ensemble ARNNx framework on the MODWT decomposed training series and economically filtered exogenous variables. Unlike typical methods, the ARNNx model does not reconstruct the economic series into an input–output supervised framework; instead, it leverages p-6 lagged observations (as we have six exogenous variables after HP and CF decomposition) of each of the decomposed training data and the previous lagged values of the exogenous variable to generate a one-step-ahead forecast using a non-linear function as given in Eq. (2) and (3). Furthermore, we iteratively update the training data with the latest forecast, developing a multi-step-ahead forecast for each transformed series and aggregating forecasts from each wavelet decomposed series for our results. Our experimental setup involves two test horizons (24 months and 12 months) and distinct training periods corresponding to each of the horizons. For the 24 months period, we consider the training data from January 2003 to November 2019 and perform the decompositions of this available training dataset. For the 12-month horizon, the training period spans from January 2003 to November 2020, and the proposed FEWNet framework is fitted into this training set. Finally, for evaluation purposes, we use the original test data from each of these forecast horizons only to report the efficiency of the proposed FEWNet framework. Therefore, there is no data leakage while decomposing the data in this paper.

4. Empirical risk minimization

FEWNet utilizes wavelet decomposition as a filtering stage and combines it with autoregressive neural networks that incorporate exogenous variables. This combination allows for precise predictions of non-stationary and non-linear time series. Wavelet decomposition yields a hierarchical structure of new time series derived from the original time series, facilitating their modeling and forecasting. This section demonstrates that FEWNet effectively minimizes the empirical risk compared to classical methods, hence highlighting its practical relevance.

Let Y_t , ($t = 1, 2, \dots, N$) be the observed time series (stationary, if random). We aim to forecast the values of $Y_{p+1}, Y_{p+2}, \dots, Y_{p+m}$ (where $m \geq 1$ is the forecast step) using p observations iteratively. In the regression

Algorithm 1: Proposed FEWNet model.

Input: Training data for the FEWNet model, including the target time series $\{Y_t, t = 1, 2, \dots, N\}$ indicating CPI inflation and exogenous series X_t comprising log-transformed EPU, and GPRC.
Output: $\hat{Y}_{N+1}, \hat{Y}_{N+2}, \dots, \hat{Y}_{N+m}; m (\geq 1)$ indicating the m -step-ahead forecast of the CPI inflation series.

Methodology:

- 1 Transform the target data vector (Y_t) into K levels by applying MODWT with Haar filter to generate a sequence of $K + 1$ uncorrelated random variables indicating the local trend and high-frequency fluctuations of the series.
 - 2 Determine the value of K as $\lfloor \log_e(N) \rfloor$, where N represents the size of the training dataset.
 - 3 To quantify the economic uncertainty parameters of inflation data, apply CF and HP filters to the exogenous variables and the target variable to generate their corresponding cyclical and trend behavior, respectively.
 - for $\tilde{k} \leftarrow 1$ to K do
 - Utilize an autoregressive neural network to model the \tilde{k} -th details series with $X_{j,t}, j = 1, 2, \dots, 6$.
 - Build a feed-forward neural network consisting of an input layer with p nodes, a hidden layer with q neurons, and an output layer.
 - Input one-lagged observation for each of the six filtered covariates along with $p - 6$ lagged values of the \tilde{k} -th details series as input to the neural network. The neural network will then pass this input via q hidden neurons and generate the forecast for the next time step.
 - Determine the value of p that minimizes the SMAPE and set $q = \lceil \frac{p+1}{2} \rceil$ (rounded to the nearest integer) for a stable learning architecture and shorter run time of the model.
 - return One-step-forward forecast of the details series.
 - 4 Apply an autoregressive neural network to both the smooth series of Y_t and the exogenous variables, following the same definition used for the details series. Use this model to generate a forecast for future values.
 - 5 Create an ensemble framework to merge the forecasts produced from several series and get the final one-step-forward prediction.
 - 6 Iteratively generate multi-step-forward forecasts.
-

setup, a functional relationship is established between Y_{p+m} and the input vector $[Y_1, Y_2, \dots, Y_p]$ by minimizing the predictive error. The optimal prediction sequence $\hat{Y}_{p+1}, \hat{Y}_{p+2}, \dots$ minimizes the generalization risk defined

as follows:

$$\mathcal{R}_{\text{Gen}} = \lim_{T \rightarrow \infty} \frac{1}{T} \sum_{p=1}^T \mathbb{E} \left[\left(\hat{Y}_{p+m} - Y_{p+m} \right)^2 | Y_p, Y_{p-1}, \dots \right], \quad (5)$$

where $\hat{Y}_{p+m} = \mathbb{E}[Y_{p+m}|Y_p, Y_{p-1}, \dots]$. However, the computation of \hat{Y}_{p+m} is difficult, as the observed time series has N observations (training samples). Therefore, we minimize the following empirical risk:

$$\mathcal{R}_{\text{Emp}} = \frac{1}{N} \sum_{i=1}^N \left(Y_i - \hat{Y}_i \right)^2, \quad (6)$$

where \hat{Y}_i is the prediction (expectations can be omitted for deterministic time series). In practical problems of economic time series forecasting, the relationship between \hat{Y}_{p+m} and the observed time sequence Y_p, Y_{p-1}, \dots is supposed to be non-linear in nature. Thus, the inclusion of autoregressive neural networks (a set of feed-forward artificial neural networks designed specifically for predicting future values in time series data) for forecasting is justified in this exercise. The relationship can be estimated by

$$\hat{Y}_{p+m} = f(Y_p, Y_{p-1}, \dots, Y_1), \quad (7)$$

where f denotes an autoregressive neural network function. The model's order (p) is an essential parameter to estimate. Smaller values of p make model training simple but miss the information about the past lagged values, whereas larger values of p compel the model training hard, resulting in the so-called curse of dimensionality. To avoid the issues of underfitting and overfitting, we use the ARNNx model, where we choose p by minimizing the SMAPE for the validation set. If f in Eq. (7) is a complex estimator (e.g., deep learning models such as transformers, deep MLP, etc.), it will learn well on the training data but perform poorly on unseen test data. The application of MODWT decomposes the time series using low- and high-pass band filters iteratively, resulting in a trend series and several detailed series (containing dynamics of the economic system at different scales). ARNNx is then trained to model the trend and detailed series and provide predictions for future values. The combined values of these MODWT-decomposed series provide a prediction of the original economic data. Although the main motivation for using wavelet decomposition on these economic time series is to enhance the predictive power, MODWT gives the smooth term S_K that contains the slowest dynamics (noise-free) and $\delta_{\tilde{k}}$ that contains system dynamics (noisy). The low-resolution data are frequently contaminated by noise. Consequently, training an ARNNx model on these time series is less challenging compared to the original time series. As \tilde{k} increases, the dynamics get slower, resulting in a low-level details series that consists solely of noise. To mitigate overfitting, one can assign a value of zero to their predictions.

Several recent works (Aminghafari & Poggi, 2007; Aussem & Murtagh, 1997; Panja, Chakraborty, Kumar et al., 2023; Soltani, 2002) have proposed treating

wavelet-decomposed time series independently. Another complicated approach is to treat each series along with other series (treated as exogenous variables), but this results in increasing the dimensionality of the time series forecasting problem. In the current formulation, we model S_K and other $\delta_{\tilde{k}}$, ($\tilde{k} = 1, 2, \dots, K$) series using ARNNx models as follows:

$$\begin{aligned} \hat{S}_{K,p+m} &= \hat{f}_0(S_{K,p}, S_{K,p-1}, \dots, S_{K,p-r_0}, \underline{X}) \text{ and} \\ \hat{\delta}_{\tilde{k},p+m} &= \hat{f}_{\tilde{k}}(\delta_{\tilde{k},p}, \delta_{\tilde{k},p-1}, \dots, \delta_{\tilde{k},p-r_{\tilde{k}}}, \underline{X}), \quad \tilde{k} = 1, 2, \dots, K. \end{aligned} \quad (8)$$

The choice of \hat{f}_i ($i = 0, 1, 2, \dots, K$) is related to the properties of the time series (non-linear, for this case). Panja, Chakraborty, Kumar et al. (2023) proposed a non-linear ARNNx model, and each \hat{f}_i may have the same order for r_i (we use r for the rest) to decrease the model's complexity. The predictions are made as an equally weighted combination of smooth and details predictions:

$$\hat{Y}_{p+m} = \hat{S}_{K,p+m} + \sum_{\tilde{k}=1}^K \hat{\delta}_{\tilde{k},p+m}. \quad (9)$$

In this context, we establish the empirical risk minimization (ERM) property for our proposed FEWNet framework. In statistical learning theory, ERM defines a family of learning models and provides theoretical bounds on their performance. This is useful, since in practice we cannot generalize how well a model will work (called true risk) because we do not know the true data distribution. However, we can instead measure its performance on a known training dataset (called empirical risk).

In FEWNet, we use ARNNx estimators $\hat{f}_0, \hat{f}_1, \dots, \hat{f}_K$ with the same order r having an equal number of neurons in the network architecture. These estimators are obtained by simultaneously minimizing the following empirical risk:

$$\mathcal{R}_{\text{Emp}}^W = \frac{1}{N} \sum_{p=1}^N \left[\left(S_{K,p+m} - \hat{S}_{K,p+m} \right) + \sum_{\tilde{k}=1}^K \left(\delta_{\tilde{k},p+m} - \hat{\delta}_{\tilde{k},p+m} \right) \right]^2. \quad (10)$$

Since ARNNx estimators can be expressed as a non-linear combination of linear projections of lagged inputs for the CPI inflation series, the following result holds:

Proposition 1. Let the autoregressive neural network (of order r) be applied to the original data (as in Eq. (7)) by minimizing the risk \mathcal{R}_{Emp} (as given in Eq. (6)). FEWNet fits the ensemble model on the decomposed data by minimizing the empirical risk $\mathcal{R}_{\text{Emp}}^W$ (as in Eq. (10)). Then, we have

$$\min \mathcal{R}_{\text{Emp}}^W \leq \min \mathcal{R}_{\text{Emp}}. \quad (11)$$

Proof. See Appendix A.4 for the detailed proof.

Remark 2. However, it by no means guarantees the generalization risk reduction. In practical scenarios, the selection of the models for $\delta_{\tilde{k},p}$ and $S_{K,p}$ is crucial and can be done using cross-validation. Also, the choice of

r_i , ($i = 0, 1, \dots, \mathcal{K}$) may change the results in practice, and this can be thought of as a future advancement of this study. Our theoretical results show the robustness of the wavelet decomposed approaches in our proposal from an ERM perspective.

5. Experimental evaluation and analysis of results

We assessed the efficacy of the proposed FEWNet framework by comparing its performance to other baseline predictions derived from statistical, machine learning, and deep learning methodologies. In our experimental evaluation, we utilize a five-fold time series cross-validation approach to train all the forecasting frameworks. We then generate forecasts for two different time horizons, specifically 12 months and 24 months, to demonstrate the generalizability of the setup. In this section, we briefly explain the baseline models (Section 5.1), evaluation metrics (Section 5.2), benchmark comparison and experimental results (Section 5.3), the statistical significance of the results (Section 5.4), empirical validation of theoretical results (Section 5.5), robustness and sensitivity analysis (Section 5.6), and conformal prediction (Section 5.7).

5.1. Baseline models

We compared the FEWNet model and various baseline models, as well as a range of machine learning and deep learning algorithms that allow for the incorporation of exogenous factors. The evaluation incorporates the following competitive models:

- Random walk (RW) is one of the simplest stochastic models based on the assumption that in each period, the time-dependent variable takes a random step away from its previous value, and the steps are independently and identically distributed in size with zero mean (Pearson, 1905). The model assumes no mean reversion, which can serve as a naive benchmark. Random walk with drift (RWD) is similar to RW but includes a constant drift term.
- The autoregressive (AR) model forecasts the variable of interest using a linear combination of the past values of the variable. It is like a multiple linear regression with p lagged values of Y_t as predictors, thus referred to as the AR(p) model (autoregressive model of order p) (Hyndman & Athanasopoulos, 2018).
- The Markov switching generalized autoregressive conditional heteroscedasticity (MSGARCH) model combines the generalized autoregressive conditional heteroskedasticity (GARCH) model with a Markov-switching process (Gray, 1996; Haas, Mitnik, & Paolella, 2004). This allows for changes in the volatility regime according to a Markov process. MSGARCH accounts for regime changes in volatility, providing a robust benchmark for comparing models in financial econometrics.
- The autoregressive integrated moving average with exogenous variable (ARIMAX) model is widely used in time series forecasting (Box & Pierce, 1970). The

ARIMAX (p, d, q) framework captures the linear patterns of the time series by considering p previous values of the target series, q prior forecast errors, and historical values of the exogenous variable. This framework employs a differencing technique of order d to guarantee the stationarity of the data. The coefficients of the linear ARIMAX model are estimated by minimizing the Akaike information criterion (AIC) value.

- Seasonal ARIMAX (SARIMAX) is an extension of the ARIMAX model for seasonal time series datasets. The model has a similar architecture as the ARIMAX model, with additional parameters for modeling the linear trend in the seasonal components of the series. Thus, the SARIMAX ($p, d, q)(P, D, Q, s$) framework models the non-seasonal components of time series with parameters (p, d, q) , and for the seasonal components of length s , it utilizes the parameters (P, D, Q, s) (Hyndman & Khandakar, 2008).
- The autoregressive fractionally integrated moving average with exogenous variable (ARFIMAX) model generalizes the classical ARIMAX model by allowing the value of the differencing parameter d to be a fraction, i.e., $d \in (-0.5, 0.5)$. The ARFIMAX (p, d, q) process has been widely studied to model and forecast time series exhibiting long-range dependence (Granger & Joyeux, 1980). As evident in Table 2, the CPI inflation series along with the economic uncertainty indices exhibit long-range dependency. Thus, the choice of using the ARFIMAX model seems reasonable for our analysis to account for slowly decaying auto-correlations.
- The deep-learning-based autoregressive (DeepAR) model is an advanced deep learning system designed specifically for forecasting time series data. This framework employs a recurrent neural network architecture to forecast future trajectories in a dataset that varies over time (Salinas, Flunkert, Gasthaus, & Januschowski, 2020).
- Neural basis expansion analysis for time series (NBeats) is a dense neural network structure explicitly developed for time series prediction problems. This model consists of many blocks, each composed of two main layers (Oreshkin, Carpol, Chapados, & Bengio, 2019). The initial layer is responsible for modeling the time series to replicate previous observations and produce forecasts. Conversely, the second layer focuses on re-modeling the discrepancies between the actual and predicted values generated by the first layer and adjusting the forecasted figures. In our testing, we set the number of blocks to two to decrease the computational complexity of the framework.
- The autoregressive distributed lag (ARDL) model has been extensively employed in the field of econometrics to estimate the long-run and short-run dynamics of time series data (Pesaran, Shin, et al., 1995). The distributed lag components of the ARDL model are capable of simulating both stationary and non-stationary time series components.

- Lasso regression is a regularized linear regression model that handles overfitting using the L1 penalty. The penalty term involved in the loss function of the lasso model helps to shrink the coefficients of the regressor variables with limited predictive power, thus leading to feature selection (Li & Chen, 2014).
- Extreme gradient boosting (XGBoost) is a supervised machine learning algorithm that aims to predict the target variable through the ensemble of a set of weak learners (Chen & Guestrin, 2016). These tree-based models are trained in a sequential fashion, where the model attempts to minimize the remaining error components of all the prior trees. During prediction, the sum of all the predicted values of the weak learners is reported. In our experimental analysis, we convert the forecasting task into a supervised prediction problem where the lagged inputs and the exogenous variables are the features and the subsequent forecast is the required label for the instance.
- The temporal fusion transformer (TFT) is a deep learning time series forecasting model that leverages the multi-head attention layer to capture the complex temporal dynamics of multiple time sequences. One of the key benefits of the TFT framework is its ability to model and forecast both univariate and multivariate time series simultaneously (Lim, Ark, Loeff, & Pfister, 2021). Furthermore, the architecture is capable of incorporating additional information in the form of time-variant and static exogenous regressors. In our experimentation, we set the number of attention heads as three.
- Wavelet ARIMAx (WARIMAX) is a modified version of the ARIMAx model that uses the MODWT decomposition technique for the purpose of predicting time series data (Aminghafari & Poggi, 2007). The model breaks down the signal that changes over time into several wavelet and smooth coefficients. It then uses an ARIMAx model to make predictions based on each of these series. The multi-step forecasts are derived by aggregating these candidate forecasts for a desired horizon.
- The autoregressive neural network with exogenous variable (ARNNx) model is a generalization of the classical feed-forward neural network model for the autoregressive time series process (Faraway & Chatfield, 1998). This model utilizes previous observations of the target time series and the exogenous variables as input to the network. The ARNNx model comprises a single hidden layer positioned between the input and output layers. The ARNNx (p, k) model uses p -lagged input values from the input layers and passes them via k neurons in the hidden layer. The value of k is typically calculated by the formula $k = \lceil \frac{p+1}{2} \rceil$, where p is a given parameter. This approach helps mitigate overfitting and maintain a stable learning architecture (Hyndman & Athanassopoulos, 2018). The model gets initialized with random values and trained using the gradient descent back-propagation approach (Rumelhart et al., 1986).

5.2. Evaluation metrics

In our study, we considered five evaluation metrics to assess the performance of the proposed forecaster and the baseline models in generating the 12- and 24-month-ahead forecasts of the CPI inflation series for BRIC countries. These metrics include the root mean square error (RMSE), mean absolute scaled error (MASE), symmetric mean absolute percentage error (SMAPE), Theils' U1 measure, the median relative absolute error (MDRAE), and the median absolute percentage error (MDAPE). The mathematical expression of these metrics is provided as follows:

$$\begin{aligned} \text{RMSE} &= \sqrt{\frac{1}{m} \sum_{t=1}^m (y_t - \hat{y}_t)^2}; \\ \text{MASE} &= \frac{\sum_{t=D+1}^{D+m} |\hat{y}_t - y_t|}{\frac{m}{D-S} \sum_{t=S+1}^D |y_t - y_{t-S}|}; \\ \text{SMAPE} &= \frac{1}{m} \sum_{t=1}^m \frac{|\hat{y}_t - y_t|}{(|\hat{y}_t| + |y_t|)/2} \times 100\%; \\ \text{Theils U1} &= \frac{\sqrt{\frac{1}{m} \sum_{t=1}^m (y_t - \hat{y}_t)^2}}{\sqrt{\frac{1}{m} \sum_{t=1}^m y_t^2} \sqrt{\frac{1}{m} \sum_{t=1}^m \hat{y}_t^2}}; \\ \text{MDRAE} &= \text{median}_{t=1,\dots,m} \frac{|y_t - \hat{y}_t|}{y_t - \hat{y}_t^R}; \text{ and} \\ \text{MDAPE} &= \text{median}_{t=1,\dots,m} \frac{|y_t - \hat{y}_t|}{y_t} \times 100\%; \end{aligned}$$

where y_t is the ground truth, \hat{y}_t is the forecast of the corresponding model, \hat{y}_t^R is the naive forecast at time t , and m is the forecast horizon. By convention, the model with the lowest value of the error metric is considered the best-performing model (Hyndman & Athanassopoulos, 2018; Panja, Chakraborty, Kumar et al., 2023).

5.3. Experimental results and baseline comparison

This section focuses on the implementation and effectiveness of the proposed FEWNet architecture in forecasting the CPI inflation series of BRIC countries. In order to conduct a thorough assessment, we compare the performance of FEWNet to various cutting-edge algorithms. The FEWNet model is implemented using R statistical software. The MODWT technique is first implemented using the *modwt* function from the 'wavelets' package. This function decomposes the training data into wavelet and scaling coefficients using the pyramid algorithm with the 'haar' filter. The determination of the number of decomposition levels is done conventionally as the floor function of $\log_e(\text{length}(\text{train}))$ (Percival & Walden, 2000). In the subsequent phase, each wavelet (details) and scaling (smooth) coefficient series is modeled with trend and cycle information from the log-transformed EPU, GPRC, and CPI data obtained through economic filters. This is achieved using an ARNNx model fitted with the *nnetar* function from the 'forecast' package in R. To select the

Table 4

Model parameters: (p, k) of FEWNet for BRIC countries across different forecast horizons. The table shows optimal parameter combinations for 12-month and 24-month rolling window forecasts of CPI inflation.

Country	Algorithm	$(p, k)_{FH=12M}$	$(p, k)_{FH=24M}$
Brazil	FEWNet	(6,5)	(18,11)
Russia	FEWNet	(1,2)	(18,11)
India	FEWNet	(18,11)	(12,8)
China	FEWNet	(18,11)	(12,8)

number of inputs (p) for the individual networks, a time series cross-validation approach is applied with a search range of 1–24. Subsequently, these p inputs are processed through $k = (p + 1)/2$ hidden nodes arranged in a single hidden layer. This process generates one-step-ahead forecasts for the individual series, which are aggregated to produce the final forecast. The framework iteratively generates multi-step-ahead forecasts. The hyperparameters of the FEWNet(p, k) algorithm used in this study are summarized in Table 4. Furthermore, for implementing classical forecasters, such as AR, ARIMAX, SARIMAX, ARDL, ARFIMAX, and WARIMAX, the ‘statsmodels’ library in Python is employed. Deep learning models, including DeepAR, NBeats, and TFT, are implemented using Python’s ‘darts’ library. Machine learning frameworks like lasso and XGBoost are implemented using the ‘skforecast’ package in Python. RW and RWD are implemented using the ‘forecast’ package and ‘msgarch’ packages in R, facilitated fitting the MSGARCH model using the ‘FitMCMC’ function.

After implementing the proposed FEWNet model and other baseline architectures, we generate forecasts for the specified time horizons. Tables 5 and 6 display the performance of the models for the semi-long-term (12 months) and long-term (24 months) timeframes, respectively, using out-of-sample data. The error metrics reported in the tables indicate that, in the majority of forecasting tasks, the proposed FEWNet framework outperforms the baseline models. In the semi-long-term forecasting of Brazil, the FEWNet model significantly reduces the RMSE metric of the ARNNx model. This improvement in model performance is attributed to the application of wavelet decomposition in the FEWNet model. Other accuracy metrics support a similar conclusion. For the 12-month forecast horizon, FEWNet consistently outperforms the baseline models for Brazil datasets. In the case of Russia, stochastic AR and FEWNet remained comparative, and their forecasts closely aligned with the ground truth. In the case of India, FEWNet and RWD both outperformed all the benchmark methods by a significant margin. The only stationary time series is the CPI inflation series of China, where the AR model performs the best. However, FEWNet and NBeats remained competitive, and FEWNet obtained the lowest SMAPE amongst its peers. As the Chinese CPI inflation series demonstrates a pattern of steady state (trend-stationary), linear models perform superior to others. While the wavelet-decomposition approach is commendable for tackling structural volatility and non-stationarity, its efficacy may be restricted when applied to trend-stationary or covariance-stationary series. Consequently, it may not outperform other statistical

or machine-learning methods when used on inherently stationary series (a property that is not prevalent for most macroeconomic variables). This explains the cause of the somewhat competitive or less efficient performance of FEWNet in predicting Chinese inflation numbers. In long-term forecasting, the FEWNet architecture consistently outperforms baseline models for all countries except China and Russia. In the case of China, NBeats, DeepAR, and lasso regression produce more accurate forecasts of the CPI inflation series. For the Russia CPI inflation series, the AR model outperforms FEWNet and other benchmark methods. Throughout the experimental evaluations, the importance of wavelet transformation and the economically filtered auxiliary information becomes evident for efficiently capturing both time and frequency-level dynamics of the time series. While machine learning and deep learning models generally produce competitive performances for semi-long forecast horizons, their effectiveness diminishes significantly over the long-term horizon. In contrast, the FEWNet model consistently performs well over both horizons, demonstrating its generalizability. Additionally, the wavelet decomposition of the FEWNet approach proves to be a suitable technique for modeling time-frequency information, especially for target variables exhibiting non-stationary behavior (unlike China). Given that most economic time series follow a non-stationary trajectory, the FEWNet approach emerges as an ideal framework for their long-term forecasting even in the presence of structural volatility.

5.4. Statistical significance of the results

In this section, we assess the effectiveness of different forecasting models in terms of the statistical significance of measurement error differences using the model-agnostic multiple comparisons with the best (MCB) procedure (Koning, Franses, Hibon, & Stekler, 2005). This non-parametric test computes the average rank for each of the M forecasters based on their ex ante accuracy across D datasets, and identifies the model with the minimum average rank as the ‘best’ performing technique. The MCB test determines the critical distance (CD) for each algorithm as $\Theta_\alpha \sqrt{\frac{M(M+1)}{6D}}$, where Θ_α is the critical value of the Tukey distribution at level α , and it considers the CD of the best-performing model as the reference value for the test. Following the MCB test, we calculate the algorithm’s average rank and present the MCB test results for the RMSE metric in Fig. 4. The plot reveals that the FEWNet framework achieved the lowest mean rank of 2.75 among all competing algorithms for both forecast horizons. Therefore, it is deemed to be the best-performing model, followed by AR (5.75), XGBoost (6.25), MSGARCH (6.38), NBeats (6.50), and so forth. Furthermore, the upper limit of the critical distance for the FEWNet model (shown by the shaded area in the graphs) acts as the reference value for the test. When comparing SARIMAX, ARIMAX, and ARFIMAX to the baseline, we observe that their critical intervals are much higher than the reference value and do not coincide with FEWNet. This indicates that their forecast performance is notably

Table 5

Performance of the proposed FEWNet model in comparison to baseline forecasting techniques for 12-month-ahead forecasts with exogenous factors EPU and GPRC (best results are in **bold**).

Country	Metric	RW	RWD	AR	MSGARCH	DeepAR	ARNNx	NBeats	ARFIMAX	SARIMAX	ARIMAX	LR	ARDL	XGBoost	TFT	WARIMAX	Proposed FEWNet
Brazil	RMSE	4.13	4.29	3.80	3.59	3.41	2.23	2.95	4.67	2.37	2.69	2.19	3.26	2.40	5.41	3.13	1.30
	MASE	6.16	6.40	5.58	5.19	5.24	3.32	4.41	7.49	3.77	4.29	3.45	5.57	3.62	8.51	4.88	1.80
	SMAPE (%)	52	55	45	41	37	25	34	68	29	33	26	52	27	85	39	12
	Theil's U ₁	0.33	0.35	0.30	0.28	0.20	0.14	0.22	0.38	0.16	0.19	0.14	0.25	0.17	0.48	0.23	0.09
	MDRAE	7.18	7.44	6.59	5.36	4.42	2.45	5.22	3.88	3.84	4.44	3.70	5.24	4.41	9.26	5.45	1.97
	MDAPE	0.47	0.49	0.43	0.36	0.30	0.20	0.34	0.59	0.27	0.30	0.23	0.40	0.26	0.46	0.39	0.10
Russia	RMSE	2.14	2.49	0.99	1.14	2.00	4.16	2.49	12.68	6.65	7.80	4.45	3.65	6.21	3.87	3.72	0.88
	MASE	5.04	5.87	1.95	2.31	4.66	10.17	5.63	33.84	17.62	20.26	11.28	9.67	16.06	9.96	9.44	2.21
	SMAPE (%)	33	40	11	13	26	46	38	100	69	76	48	44	63	81	44	13
	Theil's U ₁	0.19	0.23	0.08	0.09	0.15	0.25	0.23	0.50	0.34	0.38	0.26	0.22	0.33	0.42	0.23	0.07
	MDRAE	4.00	4.83	1.83	2.14	4.23	10.20	5.00	40.54	18.31	23.76	12.70	12.14	15.49	7.57	9.15	2.88
	MDAPE	0.27	0.33	0.08	0.12	0.33	0.51	0.32	1.97	1.05	1.22	0.71	0.57	0.99	0.59	0.56	0.11
India	RMSE	0.99	0.91	1.23	2.18	3.55	1.69	1.09	1.86	2.27	2.31	2.46	1.88	1.69	1.67	1.19	0.88
	MASE	1.53	1.34	2.09	3.68	6.61	2.68	1.82	2.92	3.72	3.88	4.19	2.96	3.07	2.35	2.00	1.41
	SMAPE (%)	16	15	21	33	52	33	22	28	51	54	58	38	38	24	23	15
	Theil's U ₁	0.10	0.09	0.12	0.19	0.27	0.21	0.12	0.17	0.29	0.30	0.33	0.23	0.21	0.16	0.13	0.09
	MDRAE	1.51	0.81	2.66	4.90	9.18	2.18	1.70	2.43	3.91	5.16	4.26	2.37	3.93	1.86	2.46	1.22
	MDAPE	0.15	0.11	0.23	0.35	0.68	0.26	0.20	0.38	0.30	0.34	0.44	0.30	0.36	0.15	0.22	0.15
China	RMSE	1.58	1.71	0.82	1.75	1.33	2.01	0.90	10.45	4.54	5.21	2.35	3.34	0.99	2.11	4.85	1.70
	MASE	2.02	2.19	1.07	2.40	1.73	2.76	1.18	15.68	6.68	7.67	3.24	4.75	1.25	2.77	7.18	1.93
	SMAPE (%)	173	174	103	107	94	111	116	171	146	150	115	132	99	153	149	85
	Theil's U ₁	0.94	0.95	0.42	0.46	0.42	0.49	0.34	0.83	0.68	0.71	0.53	0.62	0.35	0.80	0.70	0.43
	MDRAE	2.28	2.44	1.10	2.41	1.29	2.60	1.28	15.94	7.27	8.04	3.41	5.17	1.25	3.95	7.38	1.75
	MDAPE	1.34	1.46	0.76	2.42	1.66	1.70	0.87	14.68	6.80	7.67	2.26	5.07	0.93	1.99	7.21	0.99

Table 6

Performance of the proposed FEWNet model in comparison to baseline forecasting techniques for 24-month-ahead forecasts with exogenous factors EPU, and GPRC (best results are in **bold**).

Country	Metric	RW	RWD	AR	MSGARCH	DeepAR	ARNNx	NBeats	ARFIMAX	SARIMAX	ARIMAX	LR	ARDL	XGBoost	TFT	WARIMAX	Proposed FEWNet
Brazil	RMSE	3.56	3.93	2.73	2.78	6.16	3.56	3.11	4.27	4.13	4.49	3.67	2.86	2.56	3.58	4.11	2.31
	MASE	5.34	5.89	4.34	4.64	11.45	6.68	5.10	6.04	7.67	8.27	6.93	5.23	3.62	6.11	5.93	4.12
	SMAPE (%)	50	57	40	42	91	57	47	58	64	69	58	47	40	55	57	39
	Theil's U ₁	0.37	0.43	0.25	0.25	0.45	0.27	0.29	0.47	0.32	0.36	0.27	0.23	0.21	0.31	0.45	0.19
	MDRAE	5.11	4.52	2.63	2.97	12.66	6.81	5.60	3.67	9.31	8.31	7.49	5.87	5.11	6.85	3.76	4.84
	MDAPE	0.41	0.40	0.38	0.42	0.86	0.60	0.48	0.36	0.56	0.65	0.70	0.44	0.41	0.50	0.39	0.36
Russia	RMSE	2.06	2.74	1.03	1.82	3.26	6.12	5.26	11.69	9.90	9.49	6.97	6.67	2.16	2.72	5.22	2.24
	MASE	4.87	6.40	2.67	4.63	8.39	18.32	14.63	35.12	28.78	27.25	20.31	19.75	5.10	7.00	15.03	5.28
	SMAPE (%)	34	48	20	32	51	81	66	112	101	98	84	84	36	44	72	27
	Theil's U ₁	0.23	0.33	0.10	0.16	0.28	0.38	0.34	0.54	0.51	0.50	0.42	0.40	0.25	0.24	0.35	0.18
	MDRAE	4.58	5.80	2.12	4.71	8.29	21.94	15.12	41.21	30.43	26.85	24.53	24.47	4.76	7.21	17.53	3.51
	MDAPE	0.33	0.43	0.20	0.27	0.44	1.33	1.09	2.49	2.02	1.87	1.38	1.47	0.35	0.43	1.14	0.38
India	RMSE	3.72	3.73	2.92	1.92	1.86	2.22	4.18	2.72	2.16	2.02	2.36	2.53	1.95	6.17	2.35	1.04
	MASE	6.20	6.21	4.87	2.77	2.68	2.90	5.83	4.20	3.02	2.83	3.61	2.98	2.80	9.48	3.39	1.49
	SMAPE (%)	51	51	43	26	26	35	46	38	34	31	47	37	33	65	37	17
	Theil's U ₁	0.26	0.26	0.21	0.15	0.15	0.23	0.29	0.21	0.21	0.19	0.26	0.26	0.20	0.37	0.21	0.10
	MDRAE	10.76	10.80	8.25	3.71	3.25	4.31	6.22	6.46	4.02	4.07	4.21	2.12	4.28	13.47	3.70	1.42
	MDAPE	0.70	0.70	0.54	0.24	0.31	0.24	0.49	0.42	0.30	0.28	0.41	0.21	0.26	1.07	0.40	0.14
China	RMSE	3.15	3.23	2.23	2.08	1.71	1.85	1.43	18.37	3.48	4.04	1.59	2.00	2.87	2.05	7.40	2.01
	MASE	3.95	4.06	2.74	2.63	1.95	2.15	1.75	25.72	4.23	5.05	1.89	2.33	3.12	2.42	10.17	2.37
	SMAPE (%)	101	102	89	89	81	77	77	168	102	109	75	79	115	100	139	82
	Theil's U ₁	0.45	0.46	0.36	0.35	0.40	0.34	0.27	0.81	0.48	0.51	0.30	0.34	0.65	0.46	0.64	0.36
	MDRAE	3.87	4.07	2.61	2.42	1.53	2.32	1.60	26.02	4.43	4.99	2.09	2.51	2.68	2.32	10.88	2.50
	MDAPE	1.68	1.73	1.14	0.95	0.57	0.85	0.63	11.56	2.05	2.41	0.55	0.99	1.14	0.84	4.84	0.84

worse than the FEWNet approach. The AR model obtained second place and fell short of FEWNet's performance. MSGARCH, although designed for handling volatility, does not surpass FEWNet. Our analysis underscores the statistical significance of the performance difference and the

superiority of the proposed FEWNet model across datasets and forecast horizons. Moreover, the test establishes that FEWNet consistently and significantly outperforms other baseline models, as well as various machine learning or deep learning models.

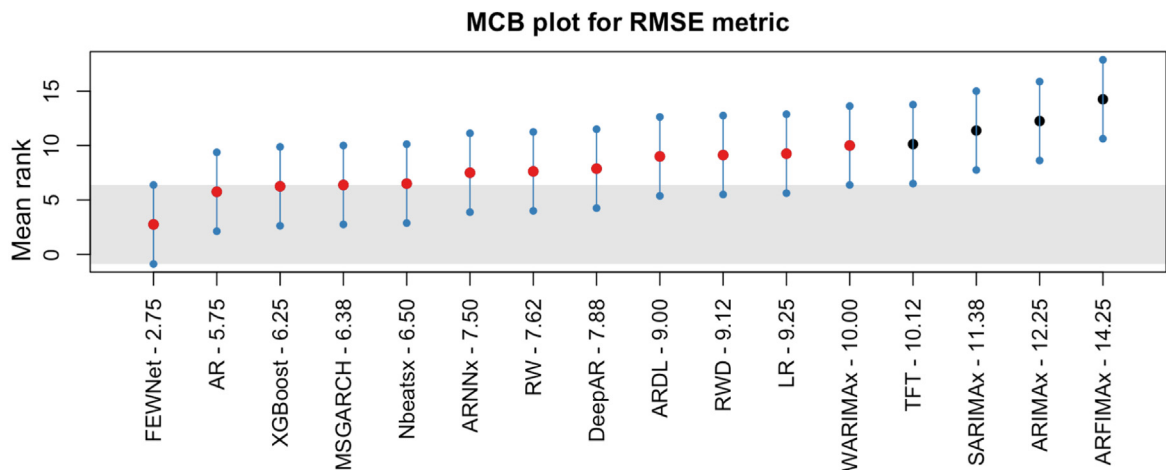


Fig. 4. Visualization of the multiple comparisons with the best (MCB) analysis for BRIC countries. In the figure, for example, 'FEWNet - 2.75' means that the average rank of the proposed algorithm FEWNet based on the RMSE error metric is 2.75; the same explanation applies to other algorithms.

In addition to the MCB test, the Giacomini and Rossi (GR) test (Giacomini & Rossi, 2010) is employed to assess the robustness and forecasting ability of the proposed FEWNet model under 'unstable environments' in comparison to other baseline models. The GR test is designed to evaluate whether one forecasting model consistently outperforms another over a specified period, particularly in data with structural breaks or regime shifts, which traditional tests like the Diebold–Mariano test might not effectively handle (Diebold & Mariano, 2002; Rossi & Sekhposyan, 2016). The GR test specifically examines the stability of relative local forecasting performance over time. We used the 'murphydiagram' package in R to perform the GR test. Based on the MCB test results, the top two baseline models identified are AR and XGBoost. We employ the GR test to further evaluate the stability of the relative predictive accuracy of these models over time. This test facilitates pairwise comparisons between FEWNet and each of the two baseline models, enabling a rigorous assessment of their relative performance. The GR test is performed at a 10% level of significance ($\alpha = 0.90$), with critical value (CV) thresholds indicated by thick black lines in the plots. The fluctuation test diagrams display varying widths of CV bounds and different endpoints for the rolling window across time. This variability can be attributed to the choice of the parameter (μ), which captures the size of the rolling window relative to the evaluation sample during the GR test implementation. The null hypothesis of the fluctuation test (GR test) posits that both forecasting methods perform equally well (with the same expected score) at all time points, while the alternative hypothesis seeks to identify whether their performance differs at any time point. The objective is to find the value of μ that helps pinpoint where the performance divergence occurs. Consequently, different forecasting methods result in different CV thresholds and rolling window sizes, reflecting the unique points of performance variation over time. These charts are based on semi-long-term (12 months)

and long-term (24 months) forecasting horizons (refer to Figs. 5 and 6). Particularly, for long-term forecast horizons (as in Fig. 6), FEWNet shows significant performance improvements around November 2021 (2021–11) compared to AR and December 2020 (2020–12) against XGBoost for the Brazil dataset. In Russia, the model demonstrates superior accuracy over AR from mid-2021, and outperforms XGBoost in a similar time frame. For India, significant performance advantages are observed around mid-2021 against AR and early 2020 against XGBoost. In China, the FEWNet model shows marked improvements over AR in late 2021 and over XGBoost in mid-2021. These findings collectively establish FEWNet as a more accurate and stable forecasting model under dynamic economic conditions, highlighting its potential as a valuable tool for economic forecasting and policy analysis. Similarly, in Fig. 5, the FEWNet model demonstrates better performance compared to the XGBoost model around October 2021 (2021–10) and shows improved performance against the AR model around November 2021 (2021–11), although it nearly crosses the CV threshold for Brazil. In Russia, FEWNet's performance is comparable to AR and XGBoost until mid-2021, where it starts to show a trend of outperforming the baselines, as indicated by the CV thresholds. For India, the fluctuation test reveals that FEWNet nearly crosses the CV threshold against both baselines around mid-2021, indicating promising performance but stopping short of significant divergence. Similarly, in China, FEWNet shows a consistent trend of outperforming the baselines, particularly against the AR model, although the differences are less pronounced. The analysis reveals that FEWNet offers very promising performance for most countries, often nearing or surpassing the baselines. However, the difference in performance is more evident over longer forecast horizons. The semi-long-term forecast horizon (12 months) provides only 12 data points, which might limit the ability of the GR test to detect significant performance differences. Additionally, the smaller sample size in the semi-long-term forecast

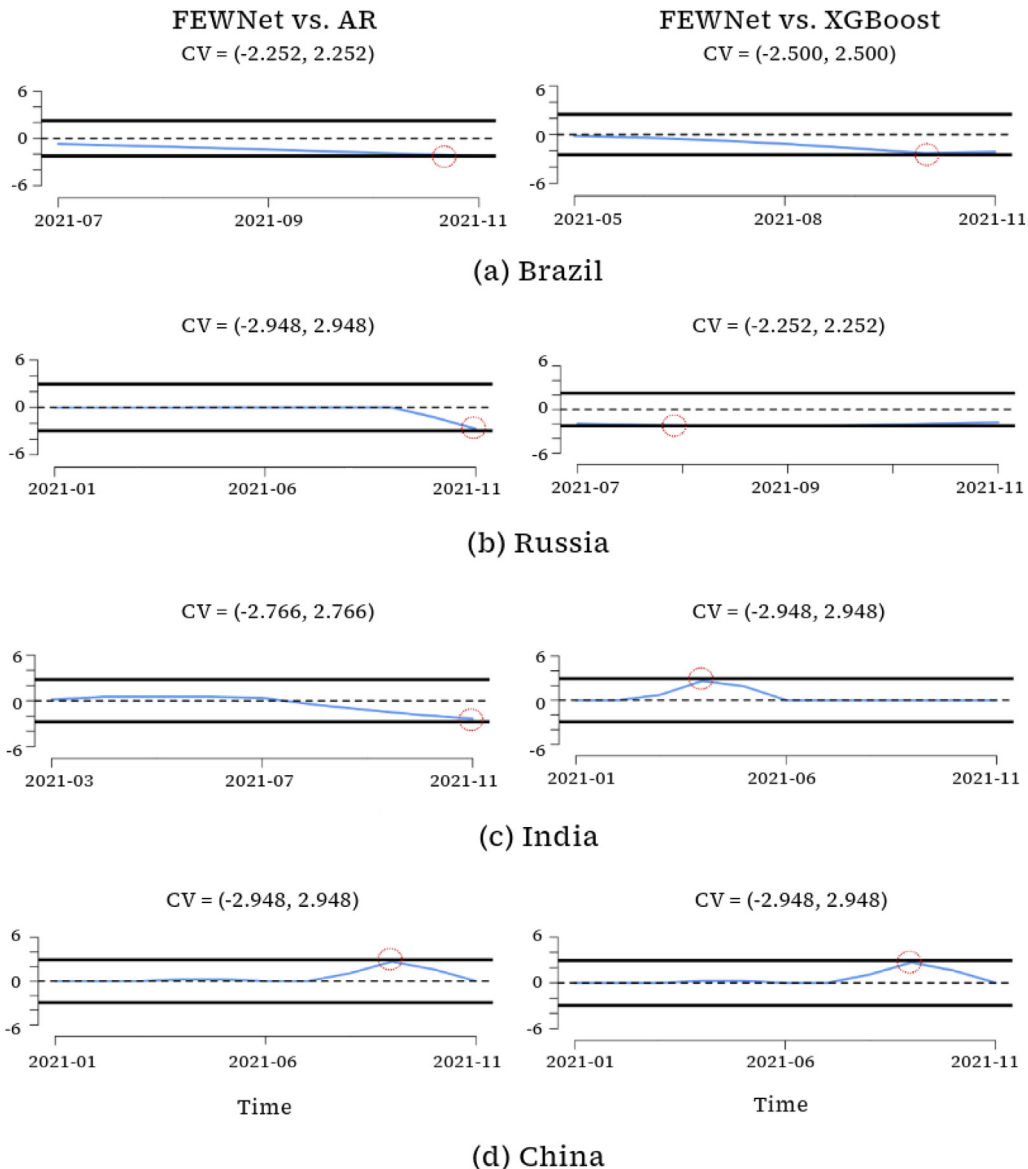


Fig. 5. Results of the GR test (Giacomini & Rossi test) of the forecasting ability of FEWNet with baselines (AR (left) and XGBoost (right)) for 12 months ahead with ($\alpha = 0.90$) for (a) Brazil, (b) Russia, (c) India, and (d) China. Points outside the CV are marked under the red dotted circles, representing that FEWNet and the other two top-performing benchmarks differ significantly. (For interpretation of the references to colour in this figure legend, the reader is referred to the web version of this article.)

may account for instances where the fluctuation test fails to identify points where the line almost crosses the CV but stops early. This analysis underscores FEWNet's robustness and effectiveness at inflation forecasting under economic policy and geopolitical uncertainties, particularly over extended periods. From the GR test, we can conclude that the proposed FEWNet model consistently outperforms the top-performing baseline models (AR and XGBoost) across BRIC countries during test periods. These findings collectively establish FEWNet as a more accurate and stable forecasting model under dynamic economic conditions, highlighting its potential as a valuable tool for economic forecasting and policy analysis.

5.5. Empirical results on ERM

We investigate the empirical risk of the proposed FEWNet model on BRIC datasets (training series). Empirically, ERM helps to improve the model's accuracy by minimizing the empirical risk and reducing the level of error or deviation between the predicted and actual values of the dataset. The key challenge in the inflation series is to learn fast dynamics and to cancel the noise simultaneously. We tackle this problem by iterative application of wavelet decomposition using low- and band-pass filters, resulting in a trend series and a hierarchy of details series that contains the system's dynamics

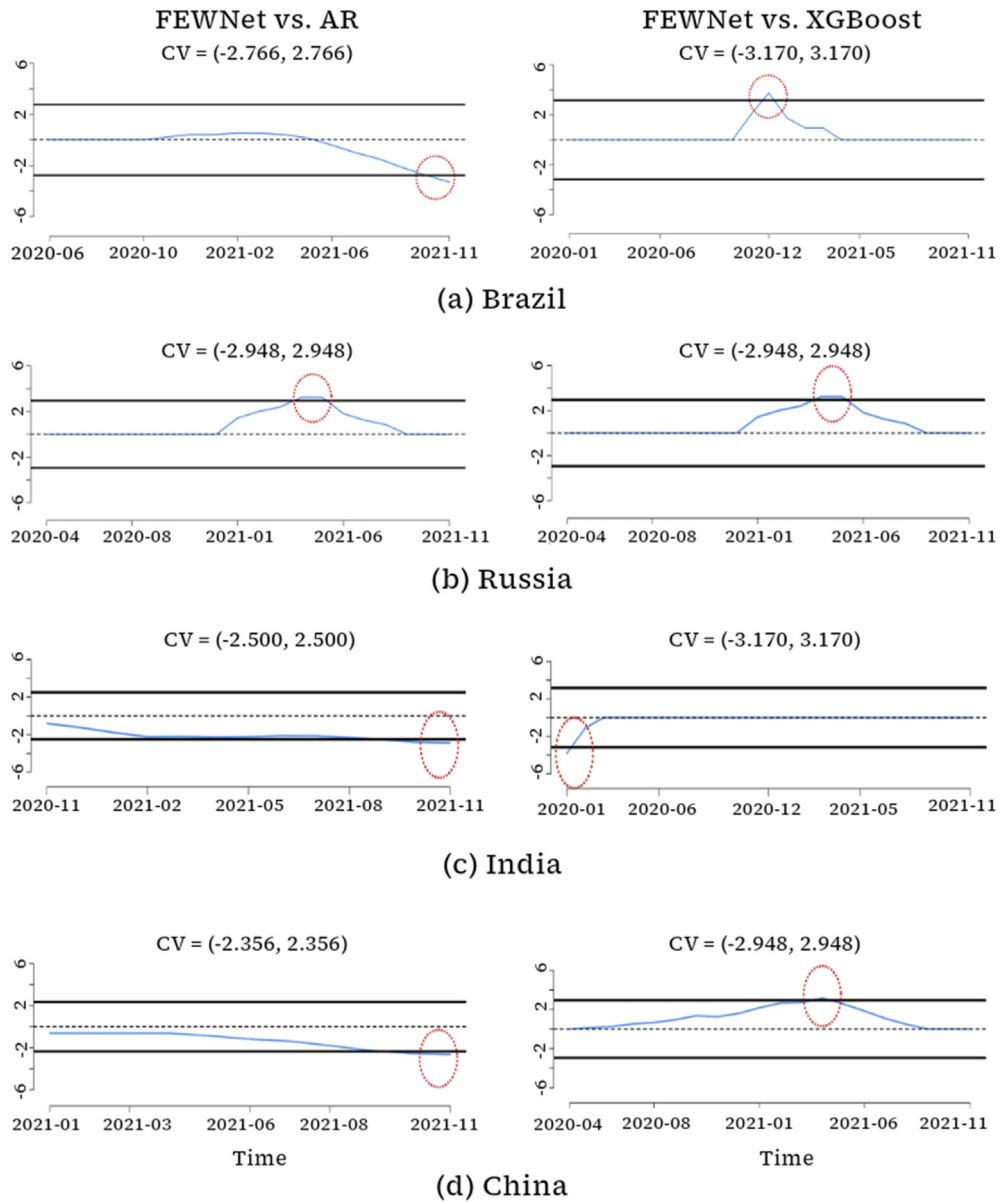


Fig. 6. Results of the GR test (Giacomini & Rossi test) of the forecasting ability of the FEWNet with baselines (AR (left) and XGBoost (right)) for 24 months ahead with ($\alpha = 0.90$) for (a) Brazil, (b) Russia, (c) India, and (d) China. Points outside the CV are marked under the red dotted circles, representing that FEWNet and the other two top-performing benchmarks differ significantly. (For interpretation of the references to colour in this figure legend, the reader is referred to the web version of this article.)

at different scales. Several ARNNx are trained to model these decomposed series and provide forecasts of the original time series by combining individual forecasts. We theoretically proved in Section 4 that using the FEWNet method (incorporated wavelet decomposition) reduces the empirical risk under some conditions. We now carry out practical experiments on BRIC countries' datasets to show that the use of the wavelet coefficients is robust to model estimation and reduces the generalization risk for the majority of the training samples, as depicted in Table 7. It is clear from Table 7 (in-sample predictions)

that FEWNet has improved performance for highly non-stationary time series as compared to standard neural networks and other benchmarks as well as for out-of-sample forecasts, as depicted in Tables 5 and 6. This has a series of practical implications and is important in policymaking. In an ideal situation, FEWNet will always perform better than the autoregressive neural network model. Also, as FEWNet can separate the fast dynamics from the slow ones and generate a combined forecast, it escapes the problem of underfitting and overfitting. Thus,

Table 7

Empirical risk comparison of two different training periods (best results are in **bold**).

Training period	Models	Brazil	Russia	India	China
2003-01 to 2020-11	ARNNx	2.61	16.62	0.51	1.16
	FEWNet	1.14	0.77	1.38	1.10
2003-01 to 2019-11	ARNNx	5.79	17.66	0.54	1.23
	FEWNet	4.60	13.13	0.93	1.01

FEWNet is more suitable for countries with complex, non-stationary CPI inflation time series and will be very useful for policymakers at central banks in BRIC countries to easily visualize the future path of inflation. A more detailed discussion on policy implications is given in Section 6.

5.6. Robustness and sensitivity analysis

This section provides a more comprehensive robustness and sensitivity analysis of the FEWNet method. For instance, we first study the impact of the HP and CF filters in the FEWNet model. This is of particular interest, since (Hamilton, 2018) criticized the HP filter for generating spurious dynamic relations and producing end-sample values that differ significantly from mid-sample values. Drehmann and Yetman (2018) rejected this criticism by highlighting scenarios in macroeconomic contexts where the HP filter is useful and robust. The HP filter is more accurate when applied to medium- and long-term cycles instead of short-term fluctuations. We employ an empirical approach to verify the importance of the HP and CF economic filters in the FEWNet model. The HP filter is used to extract trend components, whereas CF filter is employed to isolate cyclical components from the CPI inflation, EPU, and GPRC series. We examined the relevance of the HP and CF filters by comparing the experimental results of the FEWNet model with and without economic filters. Tables 8 and 9 summarize the performance of FEWNet and FEWNet without HP and CF filters (referred to as EWNet (Panja et al., 2023)) for the semi-long-run and long-run. The results indicate that these economic filters play a critical role in CPI inflation series analysis. The tables underscore the substantial improvement in predictive accuracy and robustness of the FEWNet model when economic filters are applied. This finding highlights the importance of integrating trend and cycle components using the HP and CF filters, which enhances the model's ability to capture the underlying dynamics of economic series. Consequently, the FEWNet model with economic filters proves to be a more effective tool for long-term economic forecasting in BRIC countries, addressing and overcoming the traditional criticisms of using the HP filter.

In addition, we analyze the sensitivity of the experimental results relative to the choice of different wavelet filters and the level of wavelet decomposition. The selection of wavelet filters is crucial in the overarching design of the proposed FEWNet architecture. The model employs the 'haar' wavelet transform filter to decompose the underlying CPI inflation series into detailed and smooth components. In order to rationalize the choice of the wavelet transform filter, we conduct an iterative

out-of-sample forecast evaluation, comparing the performance of these competing models (the FEWNet model with different wavelet filters) over the semi-long-term (12 months) and long-term (24 months) forecast horizons. A grid-search approach is used to determine the optimal set of hyperparameters for the underlying ARNNx model within the FEWNet framework. The selection of the wavelet decomposition level (K) is determined by the formula $K = \lfloor \log_e(N) \rfloor$, where N represents the size of the training observations (Percival & Walden, 2000). This calculation yields $K = 5$. The same decomposition level is applied uniformly to ensure a fair comparison among different wavelet filters. It is standard practice in financial forecasting exercises to utilize five to six levels of detail. For monthly data, the first detail (δ_1) captures oscillations between 2–4 months, δ_2 between 4–8 months, δ_3 between 8–16 months, δ_4 between 16–32 months, and δ_5 between 32–64 months. This approach effectively captures business cycle frequency dynamics, as additional details would require longer time period information, which is often unavailable for most macroeconomic series (Souropanis & Vivian, 2023). For a comprehensive comparison, we considered four other wavelet transform filters: (a) Daubechies with length eight (d8), known for its orthogonality and compact support and effective at capturing intricate structures in the data; (b) least asymmetric with length eight (la8), a wavelet that balances asymmetry and orthogonality, providing a more symmetric filter than Daubechies; (c) Coiflet with length six (c6), a wavelet that emphasizes both orthogonality and symmetry, making it suitable for analysis requiring smooth approximation components; and (d) the best localized with length 14 (bl14), a wavelet designed for optimal localization in both time and frequency domains, enhancing the detection of localized features in the data. The decomposition levels are uniformly set to five for all wavelet transform filters, utilizing the MODWT-based MRA approach.

Fig. 7 showcases that the FEWNet model with the 'haar' wavelet filter consistently achieves the lowest mean rank across BRIC countries, indicating its best-in-class performance among the evaluated wavelet transform filters. The rationale for the 'haar' wavelet's superior performance lies in its simplicity and capability to handle abrupt changes in data. Unlike more complex wavelets, the 'haar' wavelet's structure allows it to efficiently manage and adapt to the volatility inherent in economic series, particularly in the presence of regime shifts or exogenous shocks. This efficiency is reflected in its lower forecast errors and greater stability in predictions.

5.7. Conformalized prediction intervals

Next, we focus on quantifying the uncertainty associated with the forecast generated by the FEWNet approach using a conformal prediction interval. The non-parametric conformal prediction approach, introduced in Vovk, Gammerman, and Shafer (2005), is a set of methods that usually take an uncertainty score and turn it into a probabilistic band, including the true outcome. In other words,

Table 8

Performance comparison between the proposed FEWNet model and its variants for 12-month-ahead forecasts with exogenous factors EPU and GPRC (best results are in **bold**).

Country	Metric	FEWNet	FEWNet - d8	FEWNet - la8	FEWNet - c6	FEWNet - bl14	EWNet
Brazil	RMSE	1.30	2.76	3.10	1.36	1.93	3.63
	MASE	1.80	4.16	4.79	1.77	2.70	5.94
	SMAPE (%)	12	32	39	12	20	54
	Theil's U_1	0.09	0.19	0.22	0.09	0.13	0.28
	MDRAE	1.97	3.81	7.22	0.92	3.50	5.29
	MDAPE	0.10	0.27	0.36	0.11	0.18	0.44
Russia	RMSE	0.88	2.47	0.85	0.57	5.83	2.49
	MASE	2.21	5.90	2.16	1.29	15.48	4.88
	SMAPE (%)	13	40	13	8	63	32
	Theil's U_1	0.07	0.23	0.06	0.04	0.31	0.22
	MDRAE	2.88	4.99	2.13	1.24	16.64	3.42
	MDAPE	0.11	0.29	0.14	0.07	1.00	0.21
India	RMSE	0.88	1.41	2.73	2.15	3.59	1.77
	MASE	1.41	2.45	5.14	3.48	6.62	3.34
	SMAPE (%)	15	28	44	31	53	31
	Theil's U_1	0.09	0.15	0.22	0.19	0.28	0.16
	MDRAE	1.22	3.28	6.18	2.49	7.79	4.61
	MDAPE	0.15	0.24	0.57	0.34	0.74	0.36
China	RMSE	1.70	4.06	1.85	2.39	4.63	0.86
	MASE	1.93	5.87	2.06	3.47	6.83	1.12
	SMAPE (%)	85	138	91	123	148	105
	Theil's U_1	0.43	0.67	0.54	0.53	0.69	0.36
	MDRAE	1.75	7.06	1.16	3.57	6.20	1.00
	MDAPE	0.99	5.23	1.62	3.61	7.08	1.04

Table 9

Performance comparison between the proposed FEWNet model and its variants for 24-month-ahead forecasts with exogenous factors EPU and GPRC (best results are in **bold**).

Country	Metric	FEWNet	FEWNet - d8	FEWNet - la8	FEWNet - c6	FEWNet - bl14	EWNet
Brazil	RMSE	2.31	1.92	4.06	3.42	2.82	2.65
	MASE	4.12	3.30	7.59	6.04	4.66	4.52
	SMAPE (%)	39	34	64	52	43	41
	Theil's U_1	0.19	0.15	0.31	0.24	0.25	0.23
	MDRAE	4.84	3.14	9.31	6.12	5.51	5.12
	MDAPE	0.36	0.22	0.71	0.65	0.40	0.41
Russia	RMSE	2.24	4.84	2.94	3.56	3.81	2.90
	MASE	5.28	12.96	7.09	9.53	9.92	6.71
	SMAPE (%)	27	116	40	77	51	41
	Theil's U_1	0.18	0.55	0.24	0.39	0.28	0.23
	MDRAE	3.51	12.46	6.29	11.08	6.88	7.61
	MDAPE	0.38	0.87	0.36	0.72	0.52	0.45
India	RMSE	1.04	2.32	3.57	1.96	3.44	2.35
	MASE	1.49	3.20	5.78	2.87	5.03	2.88
	SMAPE (%)	17	44	48	26	43	26
	Theil's U_1	0.10	0.25	0.25	0.16	0.25	0.19
	MDRAE	1.42	3.55	9.58	3.85	6.44	3.24
	MDAPE	0.14	0.28	0.59	0.30	0.48	0.20
China	RMSE	2.01	2.43	2.32	1.90	2.22	3.76
	MASE	2.37	3.00	2.75	2.14	2.68	4.69
	SMAPE (%)	82	97	85	98	87	106
	Theil's U_1	0.36	0.45	0.36	0.37	0.37	0.49
	MDRAE	2.50	2.46	2.83	1.86	2.37	5.06
	MDAPE	0.84	0.99	0.91	0.71	1.07	2.18

this framework converts point estimations into a prediction region. One of the significant advantages of conformal prediction intervals is that this model-agnostic procedure guarantees coverage. In the time series setup, this method generates the prediction interval by leveraging the sequential ordering of the data. Given the training

set $\left\{Y_t, \tilde{X}_t\right\}_{t=1}^N$, where Y_t is the target series and \tilde{X}_t is the set of features, including lagged historical values of Y_t and the covariates, we fit the FEWNet framework and an uncertainty model $\hat{\Sigma}$ on \tilde{X}_t to generate a scalar notion of uncertainty. The conformal score S_t can be calculated

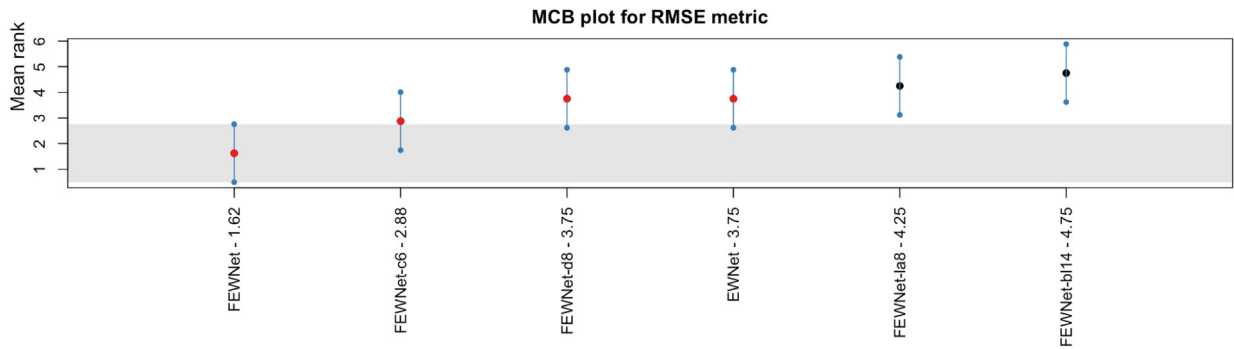


Fig. 7. Visualization of the MCB analysis for BRIC countries for different FEWNet variants of the wavelet filters along with the proposed FEWNet algorithm. In the figure, for example, 'FEWNet - 1.62' means that the average rank of the FEWNet based on the RMSE error metric is 1.62; the same explanation applies to its variants based on different wavelet filters.

as

$$S_t = \frac{|Y_t - \text{FEWNet}(\tilde{X}_t)|}{\widehat{\mathbb{E}}(\tilde{X}_t)} \quad (12)$$

Owing to the sequential nature of the data points, the conformal quantile for time series data can be calculated as a weighted conformal technique with a fixed κ -sized window $\omega_{t'} = \mathbb{1}\{t' \geq t - \kappa\}, \forall t' < t$. This now yields the quantile values as

$$\widehat{Q}_t = \inf \left\{ q : \frac{1}{\min(\kappa, t' - 1) + 1} \sum_{t'=1}^{t-1} S_{t'} \mathbb{1}(t' \geq t - \kappa) \geq 1 - \alpha \right\} \quad (13)$$

Based on these weights-adjusted quantiles, the prediction interval at each time step t can be computed as

$$\begin{aligned} & \mathbb{C}(\tilde{X}_t) \\ &= \left[\text{FEWNet}(\tilde{X}_t) - \widehat{Q}_t \widehat{\mathbb{E}}(\tilde{X}_t), \text{FEWNet}(\tilde{X}_t) + \widehat{Q}_t \widehat{\mathbb{E}}(\tilde{X}_t) \right]. \end{aligned} \quad (14)$$

In this section, we present the conformal prediction intervals for the 24 months ahead of CPI inflation forecasts generated by the FEWNet model using the validation data points (2019–12 to 2021–11). The conformal prediction interval of the FEWNet framework, calculated based on the forecast estimates and residuals for the validation set, is demonstrated in Fig. 8 along with the point estimate of the forecast produced by FEWNet and the best-performing baseline models for BRIC countries. Although the AR model ranked second based on the performance metrics, it significantly failed to capture the movements in the test CPI inflation series and may not be an effective forecasting strategy. As observed in the figure, the prediction intervals vary in width across different datasets. For instance, in the case of the 24-month forecast for Brazil, the width of the interval averages around 8.18; for Russia, it hovers around 7.93; for India, it reaches the minimum of 3.88; and for China, it averages around 7.60. A similar analysis of the conformal prediction intervals for the semi-long-term forecast horizon is provided in Appendix A.5. The overall analysis thus demonstrates a form of uncertainty quantification for the forecast of CPI

inflation series for BRIC countries and shows the structural shift in the measurement of prediction uncertainty across different countries.

6. Policy implications

Most BRIC countries, except China, have adopted inflation targeting as a framework for monetary policy, in which inflation serves as an intermediate target. Accurately forecasting inflation in such countries is essential for maintaining the credibility of these targets. By reliably forecasting inflation, central bankers in these countries can communicate their policy intentions, manage public expectations, and build trust in their commitment to price stability. However, Table 2 reveals that numerous internal and external factors influence the complex, volatile, and non-linear patterns that characterize inflation trends in BRIC countries. Two external factors that lead to such patterns are EPU and GPRC, which affect the demand or supply side of the economy (Adeosun et al., 2023), leading to large fluctuations in inflation (Balciar et al., 2017). For example, BRIC countries depend significantly on commodities such as oil, gas, and agricultural products. As a result, fluctuations in global commodity prices due to geopolitical risk can have a direct impact on inflation rates. Additionally, EPU can cause increased volatility in financial markets, affecting exchange rates and commodity prices. For BRIC countries, which are often significant commodity exporters, this can lead to fluctuating import and export prices, impacting inflation. Moreover, geopolitical tensions (e.g., the Russia–Ukraine war) can lead to economic sanctions, trade disruptions, and shifts in global economic alliances, further affecting inflation through these channels. High EPU and GPRC make it harder for central banks to set appropriate interest rates from the central banks' point of view. Reactive monetary policies may become less effective, leading to more pronounced inflation volatility and making it harder to maintain price stability (Balciar et al., 2017).

Because of how inflation, EPU, and GPRC change over time in BRIC countries, it is important for inflation forecasting models to include these uncertainty measures as exogenous variables. Ignoring them can make the forecasting process even more challenging and result in

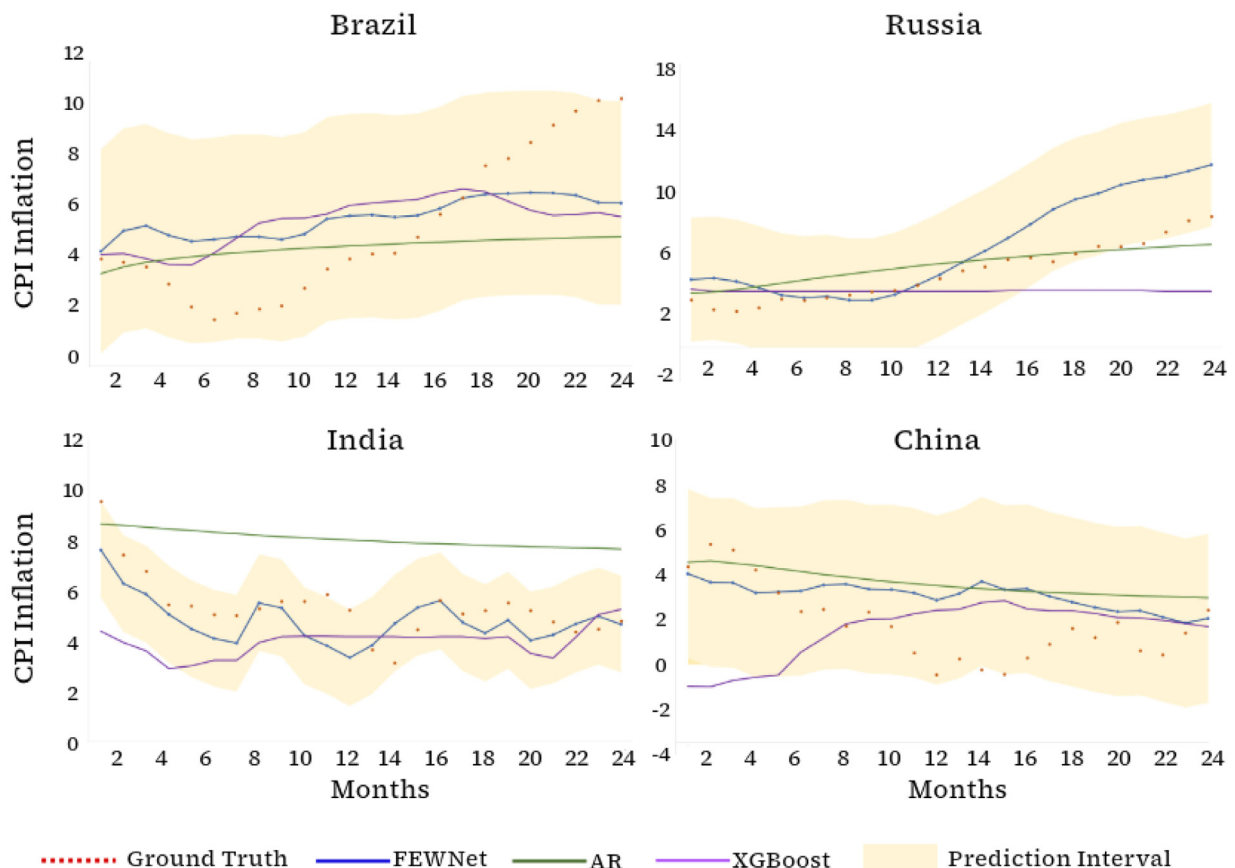


Fig. 8. The plot shows the ground truth CPI inflation data (red dots), 24-month point forecasts generated by FEWNet (blue line), AR (green line), XGBoost (purple line), and the conformal prediction interval of FEWNet (yellow shaded) for BRIC countries. (For interpretation of the references to colour in this figure legend, the reader is referred to the web version of this article.)

inaccuracies for central banks (Binder & Sekkel, 2024; Nasir, 2020). Traditional forecasting models often struggle to adapt to sudden changes and capture the non-linear dynamics characteristic of these environments. In contrast, machine learning models, particularly ensemble models, offer significant advantages for inflation forecasting in uncertain times due to their ability to process vast amounts of data and identify complex patterns (John, Singh, & Kapur, 2020; Medeiros et al., 2021).

In this paper, by employing the wavelet coherence analysis, we showed that a significant causal relationship exists between inflation, EPU, and GPRC in BRIC countries. Excluding them in the inflation forecasting models will lead to model misspecification, resulting in incorrect forecasts.² This is because the transmission channels of inflation and monetary policy change significantly during periods of high EPU (such as the global financial crisis

(GFC) of 2007–2009) and GPRC (Benchimol, 2016). Specifically, Benchimol (2016) examined the role of money and monetary policy in Israel from 2001 Q1 to 2013 Q3, particularly focusing on the GFC period. They found that substantial variability and structural changes marked the role of money and monetary policy on inflation during and after the GFC. The short-run impacts of monetary policy shocks on inflation variability were significant, especially during the subprime crisis. In the long run, however, the central bank's influence on inflation fluctuations remained critical, aligning with the Bank of Israel's objective of maintaining effective monetary policy. Further, the GFC led to structural changes in how money and monetary policy affected output and inflation, with money demand shocks playing a crucial role during crises. Given the significant variability and structural changes observed during and after the GFC, Benchimol (2016) suggested that policymakers at the Bank of Israel adopt a more flexible monetary policy framework. This framework should involve re-estimating their monetary policy models at regular intervals to monitor parameter changes, enabling quick adjustments to unexpected economic shocks and changing economic conditions to maintain price stability and support economic growth. Benchimol and El-Shagi (2020) further support this argument by examining the

² For instance, during both the global financial crisis and the Covid-19 pandemic, central banks in advanced economies experienced significant forecasting errors, notably underestimating inflation (Alessi, Ghysels, Onorante, Peach, & Potter, 2014). Researchers at the European Central Bank identified a major cause for these errors: the neglect of various financial and uncertainty indicators and the failure to account for non-linear dynamics in forecasting models (Kenny & Morgan, 2011).

impact of terrorism on inflation forecasting performance, with a particular focus on the role of monetary policy in Israel. They found that incorporating terrorism-related variables into inflation forecasting models significantly improves prediction accuracy in Israel. By accounting for terrorism, policymakers can better understand inflation dynamics and enhance the effectiveness of monetary policy, which is crucial for maintaining price stability amid geopolitical risks. Moreover, *Aastveit, Natvik, and Sola (2017)* found that economic policy uncertainty considerably affects monetary policy effectiveness, as uncertainty can dampen the response of output and inflation to monetary policy shocks. In sum, all these studies highlight the necessity of adjusting inflation forecasting models to account for varying levels of uncertainty and risk.

Putting these arguments forward, we showed that our proposed model, FEWNet, performed better at forecasting CPI inflation for Brazil, Russia, and India for semi-long-run and long-run horizons. Specifically, we can conclude that FEWNet is more suitable for countries where inflation is characterized by non-stationarity and non-linearity due to heightened volatility and other complex dynamics. Given these findings, we recommend that when policymakers at central banks in BRIC countries evaluate the future path of inflation, they should include uncertainty and risk variables like EPU and GPRC and adopt advanced machine learning models like the FEWNet model for more accurate inflation forecasting. By accounting for these factors, central banks can better understand and anticipate inflation dynamics during periods of high uncertainty, such as financial crises, pandemics, etc. This approach enables more effective monetary policy interventions, helping to stabilize output and inflation. Additionally, central banks should remain adaptable to structural changes in the economy, ensuring that their policies are responsive to evolving risks and uncertainties. This reduces the risk of policy errors, such as setting interest rates that are too high or too low relative to the economic context. Advanced models like FEWNet enable central banks to anticipate and respond to inflationary trends more effectively. This proactive approach facilitates timely and targeted interventions, especially in countries with complex and dynamic economic conditions, helping to stabilize inflation expectations and maintain economic stability.

7. Conclusion and discussion

This paper outlined a novel machine learning framework, namely FEWNet, that combines the MODWT process with the ARNNx model for long-term CPI inflation forecasting for BRIC countries under macroeconomic and geopolitical uncertainties. The proposed method demonstrated consistent performance for most BRIC economies for both semi-long-run and long-run forecast horizons. Since the CPI inflation data of China present stationary behavior, our proposal failed to outperform all the benchmark forecasters that work exceptionally well on stationary time series. However, it produced the most accurate performance for Brazil, Russia, and India, outperforming state-of-the-art machine learning or deep learning

algorithms. We also presented a framework for time series feature engineering using different economic filters (HP and CF band-pass filters) that have been leveraged in the proposed architecture, which supports the inclusion of exogenous regressors within its flexible design. A combination of the multi-resolution analysis and autoregressive neural networks is used to predict non-linear, non-stationary, and non-Gaussian time series of inflation. MODWT decomposition produces a trend time series and multiple-detail series that contain system and slow dynamics, which easily separate signal from noise. Each time series is further modeled with ARNNx. Both theoretically and empirically, we showed that under certain conditions, the proposed FEWNet reduces the empirical risk, resulting in improved forecast accuracy.

While FEWNet is designed here to predict CPI inflation in BRIC countries, its flexible framework allows for seamless adaptation to other developed countries, including OECD countries, and the inclusion of various additional uncertainty variables like Twitter (X)-based uncertainty measures, financial stress indicators, and broader indices like the World Uncertainty Index. This can be considered future research for this study. Moreover, the FEWNet framework is not limited to inflation forecasting alone. It holds significant potential for forecasting a wide array of macroeconomic variables like gross domestic product, gold prices, and unemployment rates. Its strength lies in effectively handling non-stationary and non-linear time series, which are common in macroeconomic contexts. Given its capabilities, FEWNet presents itself as a robust alternative for central banks and policymakers, which often require accurate forecasts in complex economic environments. In light of our results, further analysis of the FEWNet's performance at predicting other macroeconomic time series as well as inflation in a multivariate forecasting setting seems to be a promising avenue for future research.

Data and code availability statement

The datasets and the codes for implementing the proposed FEWNet model are made available at <https://github.com/ctanujit/FEWNet>.

CRedit authorship contribution statement

Shovon Sengupta: Writing – original draft, Visualization, Validation, Software, Resources, Investigation, Formal analysis, Data curation, Conceptualization. **Tanujit Chakraborty:** Writing – review & editing, Writing – original draft, Supervision, Software, Project administration, Methodology, Conceptualization. **Sunny Kumar Singh:** Writing – review & editing, Supervision, Resources, Investigation, Data curation, Conceptualization.

Declaration of competing interest

The authors declare that they have no known competing financial interests or personal relationships that could have appeared to influence the work reported in this paper.

Acknowledgment

The authors would like to acknowledge the Associate Editor and two experienced reviewers for insightful suggestions that improved the paper. The authors want to thank Madhurima Panja of IIIT Bangalore, India, for the discussion and help with the graphics presented in this manuscript.

Appendix

A.1. Discrete wavelet transformation

The FEWNet framework leverages a form of discrete wavelet transformation (DWT) to first denoise the CPI inflation series for BRIC countries and then model the resulting components with the auxiliary information (trend and cycle generated through HP and CF filters) using ARNNx (Faraway & Chatfield, 1998) in an ensemble setup. In particular, we focus on the 'maximal overlapping' version of the DWT popularly known as MODWT. In the literature, the DWT framework has been widely used in various applications for compressing digital images, smoothing signals (Percival & Walden, 2000; Walden, 2001), materials science (Li et al., 2020), atmosphere (Percival & Mofjeld, 1997), energy (Yang & Wang, 2021), economics, and geophysics (Zhu, Wang, & Fan, 2014), among many others. We begin with a brief description of the DWT approach that forms the mathematical basis of the MODWT used in our proposed FEWNet framework.

The DWT approach defines a class of orthogonal wavelet transformation (Percival & Guttorm, 1994). Let $\{h_l; l = 0, 1, \dots, L-1\}$ denote a finite-length discrete high-pass (wavelet) filter such that it satisfies the unit energy assumptions and sums up to zero:

$$\sum_{l=0}^{L-1} h_l^2 = 1 \text{ and } \sum_{l=0}^{L-1} h_l = 0. \quad (15)$$

Furthermore, the wavelet filters are restricted to be orthogonal to even shifts. Thus mathematically, we can denote this as

$$\sum_{l=0}^{L-1} h_l h_{l+2\tilde{n}} = 0 \text{ for any non zero integer } \tilde{n}. \quad (16)$$

Alongside the high-pass filter, having a low-pass (scaling) filter $\{g_l; l = 0, 1, \dots, L-1\}$ is also crucial for decomposing an observed time series into high-frequency oscillations and low-frequency details. These scaling filters also satisfy the unit energy assumptions and are orthogonal to even shifts (as in Eqs. (15) and (16)). Furthermore, for all the wavelet filters, the low-pass filter coefficients are determined by the quadrature mirror relationship: $g_l = (-1)^{l+1} h_{L-1-l}$ or $h_l = (-1)^l g_{L-1-l}; l = 0, 1, \dots, L-1$.

For the construction of DWT coefficients from a given series, the use of the pyramid algorithm is prevalent (Percival & Guttorm, 1994; Percival & Walden, 2000). Suppose we denote the economic time series to be transformed as $Y = \{Y_t, t = 1, 2, \dots, N\}$ of length ($N = 2^K$). In the pyramid algorithm, given the series Y , the wavelet filters

h_l , and the scaling filters g_l , the first iteration performs a down-sampling operation and convolutes the data vector with each of the filters to obtain the resulting wavelet and scaling coefficient. In the subsequent step, similar down-sampling and convolution take place on the scaling coefficients of the previous step. Following this procedure iteratively, the \tilde{k} -th stage output of the pyramid algorithm can be expressed as

$$\varpi_{k,t} = \sum_{l=0}^{L_{\tilde{k}}-1} h_{\tilde{k},l} Y_{2^{\tilde{k}}(t+1)-l \bmod N} \text{ and } v_{\tilde{k},t} = \sum_{l=0}^{L_{\tilde{k}}-1} g_{\tilde{k},l} Y_{2^{\tilde{k}}(t+1)-l \bmod N}, \quad (17)$$

where $\varpi_{k,t}$ and $v_{\tilde{k},t}$ are the \tilde{k} th ($\tilde{k} = 1, 2, \dots, K$)-level wavelet and scaling coefficients, respectively. This procedure can be repeated up to $\log_2(N)$ times. Thus, using the DWT on the given time series, we can represent the discrete wavelet coefficients in matrix notation as

$$\varpi = \mathcal{W}Y, \quad (18)$$

where \mathcal{W} , an orthogonal matrix of order $N \times N$, comprises wavelet and scaling filters arranged row by row. The wavelet coefficients ϖ can be arranged into $K+1$ vectors as $\varpi = [\varpi_1, \varpi_2, \dots, \varpi_K, v_K]^T$ with each $\varpi_{\tilde{k}}$, ($\tilde{k} = 1, 2, \dots, K$), a vector of length $N/2^{\tilde{k}}$, consisting of the wavelet coefficients associated with changes on a scale of length $2^{\tilde{k}-1}$. The vector v_K of length $N/2^K$ is associated with averages on a scale of length 2^{K-1} .

Although the DWT is a useful mathematical tool for decomposing discrete time series into simpler parts using high-pass and low-pass filters, it suffers from certain serious limitations. To begin with, the DWT approach down-samples the signal at each iteration, and it can be repeated for a maximum of $\log_2(N)$, thus restricting the size of the signal to be an exact power of 2. Moreover, the wavelet and scaling coefficients generated from a DWT convoluted signal do not scale and are not shift-invariant. This restricts the universal application of the DWT algorithm for arbitrary time series. To overcome these deficiencies of the DWT framework, a modified maximal overlapping version of DWT was proposed (Percival & Guttorm, 1994; Percival & Walden, 2000; Walden, 2001).

A.2. MODWT approach

The maximal overlapping discrete wavelet transform (MODWT) is an improved, non-subsampled version of the DWT framework. The MODWT overcomes the limitations of the DWT approach and is invariant to circular shifts. This non-decimated wavelet transform is suitable for handling the non-stationary behavior of a discrete-time process and is highly redundant. Moreover, the variance estimator pertaining to the MODWT process is asymptotically more efficient than that of the DWT (Percival & Guttorm, 1994). Thus in our study, we utilize the transition and time-invariant (Pesquet, Krim, & Carfantan, 1996) MODWT transformation for denoising the CPI inflation series. The mathematical formulation of the MODWT algorithm can be extended from the DWT approach and is described below.

For the MODWT algorithm, we define the rescaled version of filters as $\tilde{h}_l = h_l/2^l$ and $\tilde{g}_l = g_l/2^l$ and employ the pyramid algorithm with the time series Y , wavelet filter \tilde{h}_l , and scaling filter \tilde{g}_l . Similar to the DWT approach in the non-decimated MODWT framework, the pyramid algorithm convolves the data with the re-normalized filters and generates the resulting coefficients of length \mathcal{N} as

$$\tilde{\omega}_{\tilde{k},t} = \sum_{l=0}^{L_{\tilde{k}}-1} \tilde{h}_{\tilde{k},l} Y_{(t+1)-l \bmod \mathcal{N}} \quad \text{and} \quad \tilde{v}_{\tilde{k},t} = \sum_{l=0}^{L_{\tilde{k}}-1} \tilde{g}_{\tilde{k},l} Y_{(t+1)-l \bmod \mathcal{N}}, \quad (19)$$

where $L_{\tilde{k}} = (2^{\tilde{k}} - 1)(L - 1) + 1$. The wavelet ($\tilde{\omega}_{\tilde{k},t}$) and scaling ($\tilde{v}_{\tilde{k},t}$) coefficients obtained by decomposing the data vector Y using the MODWT approach into \mathcal{K} levels can be formulated as

$$\tilde{\omega} = \tilde{\mathcal{W}}Y \quad (20)$$

where the orthonormal matrix $\tilde{\mathcal{W}} = [\tilde{\mathcal{W}}_1, \tilde{\mathcal{W}}_2, \dots, \tilde{\mathcal{W}}_{\mathcal{K}}, \tilde{V}_{\mathcal{K}}]^T$ is made up of $\mathcal{K} + 1$ submatrices of size $\mathcal{N} \times \mathcal{N}$ with $\tilde{\mathcal{W}}_{\tilde{k}}$, ($\tilde{k} = 1, 2, \dots, \mathcal{K}$) and $\tilde{V}_{\mathcal{K}}$ denoting circularly shifted wavelet and scaling filters, respectively. Furthermore, the wavelet and scaling coefficients can be arranged in $\mathcal{K} + 1$ vectors as $\tilde{\omega} = [\tilde{\omega}_1, \tilde{\omega}_2, \dots, \tilde{\omega}_{\mathcal{K}}, \tilde{v}_{\mathcal{K}}]^T$ in a similar manner as in Eq. (18) of DWT approach.

Following the MODWT decomposition, an additive multi-resolution analysis (MRA) of the observed time series Y can be formulated as

$$Y_t = \sum_{\tilde{k}=1}^{\mathcal{K}} d_{\tilde{k},t}, \quad (21)$$

where $d_{\tilde{k},t}$, $t = 1, 2, \dots, \mathcal{N}$ is the t th element of $d_{\tilde{k}} = \tilde{\mathcal{W}}_{\tilde{k}} \tilde{\omega}_{\tilde{k}}$, ($\tilde{k} = 1, 2, \dots, \mathcal{K}$). Thus, the time series Y can be expressed as a linear combination of the high-frequency and low-frequency coefficients:

$$Y_t = S_{\mathcal{K},t} + \sum_{\tilde{k}=1}^{\mathcal{K}} \delta_{\tilde{k},t}, \quad (22)$$

where $S_{\mathcal{K},t} = \sum_{j=\tilde{k}+1}^{\mathcal{K}+1} d_{j,t}$ is the \mathcal{K} -level smooth coefficient, and $\delta_{\tilde{k},t} = \sum_{j=1}^{\tilde{k}} d_{j,t}$ denotes \tilde{k} -level details associated with the MODWT-based MRA decomposition. A salient feature of this scale-based additive transformation is that the wavelet and scaling coefficients of the series are associated with the zero-phase filters. Hence, they are of the same size as the original series and are perfectly aligned with it. A more detailed structural overview of the MODWT process can be found in Percival and Mofjeld (1997).

A.3. Economic filters: Hodrick–Prescott and Christiano–Fitzgerald filters

The Hodrick–Prescott filter is a popular econometric method that has found profound applications in extracting the business cycle components and as a detrending method for financial time series (Hodrick & Prescott, 1997). The method is named after its proponents: Robert

J. Hodrick and Edward C. Prescott. This nonparametric method is widely adopted by economists in central banks, international economic agencies, industry, and in government (Phillips & Shi, 2019). There is a wide array of time series filters commonly used in macroeconomic and financial research and analysis to decompose the overall time series into trend, cycle, and irregular components (Gençay, Selçuk, & Whitcher, 2001). Among them, the HP filter has been in vogue among researchers for extracting trend and cycle components from the time series. One key aspect of the HP filter is that it is quite effective and can be applied to non-stationary time series. Therefore, it is an excellent choice for decomposing CPI inflation, EPU, and GPRC series in this exercise.

For any time series data $(Y_t : t = 1, \dots, n)$, the HP filter decomposes the series into a trend (τ_t) and a cyclical component (C_t) by solving the following minimization problem with respect to τ_t :

$$\hat{\tau}_t^{HP} = \underset{\tau_t}{\operatorname{argmin}} \left\{ \sum_{t=1}^n (Y_t - \tau_t)^2 + \theta \sum_{t=2}^n (\Delta^2 \tau_t)^2 \right\} \quad \text{and} \quad \hat{C}_t^{HP} = Y_t - \hat{\tau}_t^{HP} \quad (23)$$

where $\Delta \tau_t = \tau_t - \tau_{t-1}$, $\Delta^2 \tau_t = \Delta \tau_t - \Delta \tau_{t-1} = \tau_t - 2\tau_{t-1} + \tau_{t-2}$, and $\theta \geq 0$ is a tunable parameter that controls the extent of the penalty for fluctuations in the second differences of Y_t . In other words, it controls for the volatility in the trend component. The greater the value of θ , the more stable the trend component. The choice of θ is determined by the user. Interestingly, the residual term or deviation from the trend term ($Y_t - \hat{\tau}_t^{HP}$) is defined as the business cycle components. Thus, the HP filter can be considered a highpass filter, removing the trend components and returning high-frequency components in \hat{C}_t^{HP} . Let us assume that a time series be expressed as $Y_t = \tau_t + C_t$ (where C_t incorporates the effect of any irregular term). If C_t and the second difference of τ_t are normally and independently distributed, the HP filter is an asymptotic filter, and θ is given as the ratio of two variances: $\frac{\sigma_C^2}{\sigma_{\Delta^2 \tau}^2}$,

where Δ^2 is the second-difference operator, as defined above. One interesting property of θ is that, in the limiting case, when $\theta \rightarrow \infty$, the trend component becomes a linear time trend. In common practice, $\theta = 1600$ is used, as prescribed by Hodrick and Prescott (1997), when the HP filter is applied to quarterly U.S. economic data. For other frequencies like annual or monthly data, $\theta = 6.25$ and $\theta = 129,600$ are used as default values (Ravn & Uhlig, 2002). The cyclical or residual component derived from the HP filters has the following frequency response function (Gençay et al., 2001):

$$\mathcal{H}(f, \theta) = \frac{4\theta[1 - \cos(2\pi f)]^2}{1 + 4\theta[1 - \cos(2\pi f)]^2} \quad (24)$$

and the trend component of the HP filter is given by

$$\tau_t = \frac{\phi_1 \phi_2}{\theta} \left[\sum_{j=0}^{\infty} (A_1 \phi_1^j + A_2 \phi_2^j) Y_{t-j} + \sum_{j=0}^{\infty} (A_1 \phi_1^j + A_2 \phi_2^j) Y_{t+j} \right], \quad (25)$$

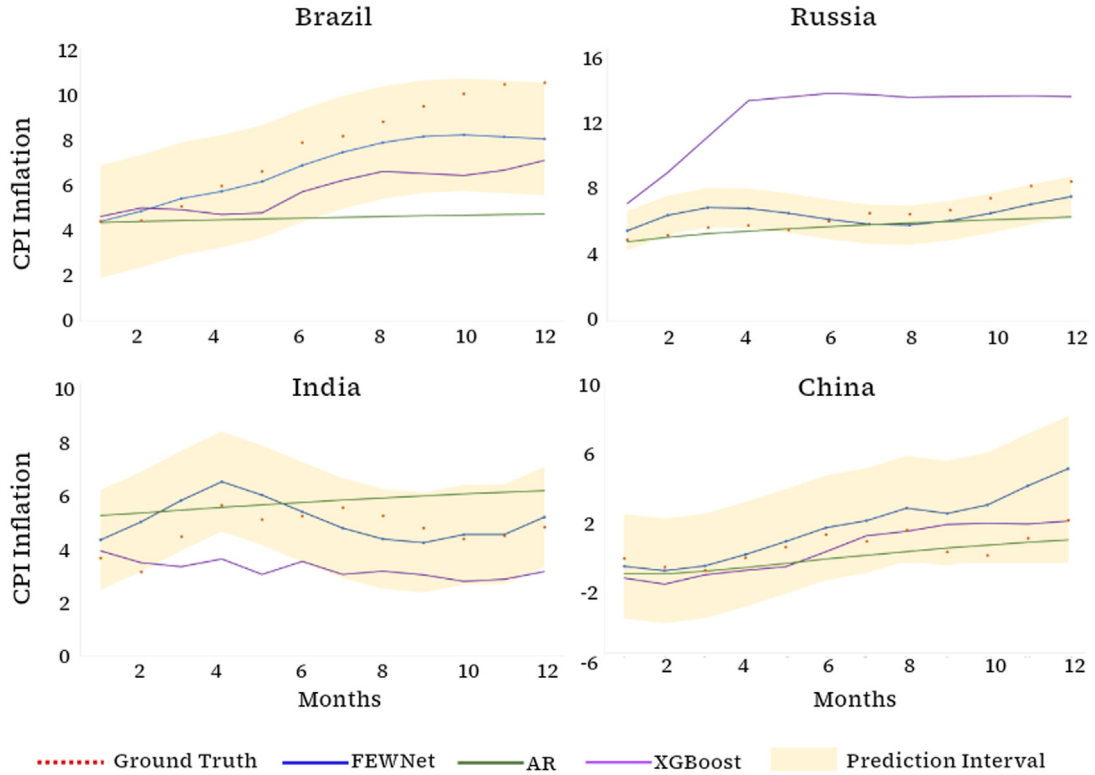


Fig. 9. The plot shows the ground truth CPI inflation data (red dots), 12-month point forecasts generated by FEWNet (blue line), AR (green line), XGBoost (purple line), and the conformal prediction interval of FEWNet (yellow shaded) for BRIC countries. (For interpretation of the references to colour in this figure legend, the reader is referred to the web version of this article.)

where ϕ_1 and ϕ_2 are the complex conjugates and depend on the value of θ and A_1 , and A_2 denotes the functions of ϕ_1 and ϕ_2 . By this analysis, it can be argued that the trend component, extracted using the HP filter, is a centered moving average term.

On the other hand, the Christiano–Fitzgerald (CF) filter (often regarded as a random walk filter) is a band-pass filter that was primarily constructed using similar principles as the Baxter and King (BK) filter (Christiano & Fitzgerald, 2003). The CF filter outperforms the BK filter in the case of real-time applications and is calculated as follows:

$$C_t = \varphi_0 Y_t + \varphi_1 Y_{t+1} + \cdots + \varphi_{T-1-t} Y_{T-1} + \tilde{\varphi}_{T-t} Y_T \\ + \varphi_1 Y_{t-1} + \cdots + \varphi_{t-2} Y_2 + \tilde{\varphi}_{t-1} Y_1 \quad (26)$$

where $\varphi_j = \frac{\sin(jb) - \sin(ja)}{\pi j}$, $j \geq 1$, $\varphi_0 = \frac{b-a}{\pi}$, $a = \frac{2\pi}{p_u}$, $b = \frac{2\pi}{p_l}$, and $\tilde{\varphi}_k = -\frac{1}{2}\varphi_0 - \sum_{j=1}^{k-1} \varphi_j$. The parameters p_u and p_l represent the break-off point of cycle length in the month. Any cycle value between p_u and p_l is preserved in the cyclical term C_t . The CF filter aims to formulate the detrending and smoothing problem in the frequency domain. The CF filter approximates the ideal infinite band-pass filter like the BK filter. One key advantage of CF filters is that the random walk filter can exploit the complete series for the calculation of each filtered point. CF filters converge well with optimal filters in the long run. This property speaks for the effectiveness of the CF filter as compared to the BK filter in the context of extracting

meaningful features (cyclical components) from a specific time series.

In this analysis, the HP filter extracts the trend component for CPI inflation, EPU, and GPRC series, whereas the CF filter extracts the cyclical terms from the three time series (CPI inflation, EPU, and GPRC). These derived features are used in the downstream FEWNet algorithm to generate the long-term forecasts for the CPI inflation series.

A.4. Proof for Proposition 1

Proof. Using Eq. (7), we write the ARNNx estimator as follows:

$$\hat{f} = \alpha + \sum_{j'=1}^{q^*} \beta_{j'} \sigma(z_{j'}) , \quad (27)$$

where $z_{j'} = \alpha^* + \sum_{i=1}^r \beta_{i,j'}^* y_i + \gamma^* \mathbf{X}$, and where the parameters are estimated by minimizing Eq. (6). For FEWNet, we have

$$\begin{aligned} \hat{f}_0 &= \alpha_0^S + \sum_{i=1}^q \beta_i^S \sigma(\alpha_i^S + \sum_{j_0=1}^r \beta_{i,j_0}^S S_{i,j_0} + \gamma_i^{S'} \mathbf{X}) \\ \hat{f}_k &= \alpha_{0,\bar{k}} + \sum_{i=1}^q \beta_{i,\bar{k}} \sigma(\alpha_{i,\bar{k}} + \sum_{j_k=1}^r \beta_{i,j_k} \delta_{i,j_k} + \gamma_{i,\bar{k}}' \mathbf{X}); \quad \bar{k} = 1, 2, \dots, K. \end{aligned} \quad (28)$$

Using Jensen's inequality and Eq. (2), we get the \mathcal{R}_{Emp} definition domain as a subspace of $\mathcal{R}_{\text{Emp}}^W$:

$$\min \mathcal{R}_{\text{Emp}}^W \leq \min \mathcal{R}_{\text{Emp}} \quad (29)$$

\hat{f} is a linear combination of \hat{f}_0 and \hat{f}_k , ($k = 1, 2, \dots, K$) with uniform weights and scaling (\tilde{g}_l). The wavelet (\tilde{h}_l) filter satisfies the unit energy assumption and even-length scaling assumption in MODWT. That is,

$$\tilde{h}_l = -\tilde{g}_l \forall l \geq 1, \quad \tilde{h}_0 + \tilde{g}_0 = 1, \quad \tilde{h}_l = \tilde{g}_l = 0 \forall l \leq -1 \quad (30)$$

Similar results may hold for any other decomposition method satisfying Eq. (30).

A.5. Conformal prediction for semi-long-term

Fig. 9 depicts the uncertainty quantification of the FEWNet framework for the 12-month-ahead forecast horizon. The conformal prediction intervals demonstrated in the figure are of varied widths across countries. In the case of 12-month forecasts for Brazil, the width of the interval averages around 5.06. For Russia, it hovers around 2.3. For India, it averages 3.7. The width value for China is around 6.03, the maximum among all the countries. This indicates a higher degree of prediction uncertainty for China than for other countries.

References

- Aastveit, K. A., Natvik, G. J., & Sola, S. (2017). Economic uncertainty and the influence of monetary policy. *Journal of International Money and Finance*, 76, 50–67.
- Adeosun, O. A., Tabash, M. I., Vo, X. V., & Anagreh, S. (2023). Uncertainty measures and inflation dynamics in selected global players: A wavelet approach. *Quality & Quantity*, 57, 3389–3424.
- Al-Thaqeb, S. A., & Algharabali, B. G. (2019). Economic policy uncertainty: A literature review. *The Journal of Economic Asymmetries*, 20, Article e00133.
- Alessi, L., Ghysels, E., Onorante, L., Peach, R., & Potter, S. (2014). Central bank macroeconomic forecasting during the global financial crisis: The European Central Bank and Federal Reserve Bank of New York experiences. *Journal of Business & Economic Statistics*, 32, 483–500.
- Alexandridis, A. K., & Hasan, M. S. (2020). Global financial crisis and multiscale systematic risk: Evidence from selected European stock markets. *International Journal of Finance & Economics*, 25, 518–546.
- Almosova, A., & Andrensen, N. (2023). Nonlinear inflation forecasting with recurrent neural networks. *Journal of Forecasting*, 42, 240–259.
- Aminghafari, M., & Poggi, J.-M. (2007). Forecasting time series using wavelets. *International Journal of Wavelets, Multiresolution and Information Processing*, 5, 709–724.
- Anderl, C., & Caporale, G. M. (2023). Asymmetries, uncertainty and inflation: Evidence from developed and emerging economies. *Journal of Economics and Finance*, 1–34.
- Araujo, G. S., & Gaglianone, W. P. (2023). Machine learning methods for inflation forecasting in Brazil: New contenders versus classical models. *Latin American Journal of Central Banking*, 4, Article 100087.
- Aussem, A., & Murtagh, F. (1997). Combining neural network forecasts on wavelet-transformed time series. *Connection Science*, 9, 113–122.
- Baker, S. R., Bloom, N., & Davis, S. J. (2016). Measuring economic policy uncertainty. *Quarterly Journal of Economics*, 131, 1593–1636.
- Balcilar, M., Gupta, R., & Jooste, C. (2017). Long memory, economic policy uncertainty and forecasting US inflation: A Bayesian VARFIM approach. *Applied Economics*, 49, 1047–1054.
- Barkan, O., Benchimol, J., Caspi, I., Cohen, E., Hammer, A., & Koenigstein, N. (2023). Forecasting CPI inflation components with hierarchical recurrent neural networks. *International Journal of Forecasting*, 39, 1145–1162.
- Becerra, V. M., Galvão, R. K., & Abou-Seada, M. (2005). Neural and wavelet network models for financial distress classification. *Data Mining and Knowledge Discovery*, 11, 35–55.
- Benaouda, D., Murtagh, F., Starck, J.-L., & Renaud, O. (2006). Wavelet-based nonlinear multiscale decomposition model for electricity load forecasting. *Neurocomputing*, 70, 139–154.
- Benchimol, J. (2016). Money and monetary policy in Israel during the last decade. *Journal of Policy Modeling*, 38, 103–124.
- Benchimol, J., & El-Shagi, M. (2020). Forecast performance in times of terrorism. *Economic Modelling*, 91, 386–402.
- Binder, C. C., & Sekkel, R. (2024). Central bank forecasting: A survey. *Journal of Economic Surveys*, 38, 342–364.
- Bloom, N. (2009). The impact of uncertainty shocks. *Econometrica*, 77, 623–685.
- Bloom, N. (2014). Fluctuations in uncertainty. *Journal of Economic Perspectives*, 28, 153–176.
- Botha, B., Burger, R., Kotzé, K., Rankin, N., & Steenkamp, D. (2023). Big data forecasting of South African inflation. *Empirical Economics*, 65, 149–188.
- Boubaker, H., Canarella, G., Gupta, R., & Miller, S. M. (2023). A hybrid ARFIMA wavelet artificial neural network model for DJIA index forecasting. *Computational Economics*, 62, 1801–1843.
- Box, G. E., & Pierce, D. A. (1970). Distribution of residual autocorrelations in autoregressive-integrated moving average time series models. *Journal of the American Statistical Association*, 65, 1509–1526.
- Caldara, D., & Iacoviello, M. (2022). Measuring geopolitical risk. *American Economic Review*, 112, 1194–1225.
- Chakraborty, T., Chakraborty, A. K., Biswas, M., Banerjee, S., & Bhattacharya, S. (2021). Unemployment rate forecasting: A hybrid approach. *Computational Economics*, 57, 183–201.
- Chen, T., & Guestrin, C. (2016). Xgboost: A scalable tree boosting system. In *Proceedings of the 22nd ACM SIGKDD international conference on knowledge discovery and data mining* (pp. 785–794).
- Chen, X., Racine, J., & Swanson, N. R. (2001). Semiparametric arx neural-network models with an application to forecasting inflation. *IEEE Transactions on Neural Networks*, 12, 674–683.
- Choudhary, M. A., & Haider, A. (2012). Neural network models for inflation forecasting: An appraisal. *Applied Economics*, 44, 2631–2635.
- Christiano, L. J., & Fitzgerald, T. J. (2003). The band pass filter. *International Economic Review*, 44, 435–465.
- Colombo, V. (2013). Economic policy uncertainty in the US: Does it matter for the euro area? *Economics Letters*, 121, 39–42.
- Crowley, P. M. (2007). A guide to wavelets for economists. *Journal of Economic Surveys*, 21, 207–267.
- Diebold, F. X., & Mariano, R. S. (2002). Comparing predictive accuracy. *Journal of Business & Economic Statistics*, 20, 134–144.
- Drehmann, M., & Yetman, J. (2018). Why you should use the Hodrick-Prescott filter—at least to generate credit gaps. *BIS Working Paper*.
- Dunis, C., & Williams, M. (2002). Modelling and trading the EUR/USD exchange rate: Do neural network models perform better? Derivatives use. *Trading and Regulation*, 8, 211–239.
- Faraway, J., & Chatfield, C. (1998). Time series forecasting with neural networks: A comparative study using the air line data. *Journal of the Royal Statistical Society. Series C. Applied Statistics*, 47, 231–250.
- Faust, J., & Wright, J. H. (2013). Forecasting inflation. vol. 2, In *Handbook of economic forecasting* (pp. 2–56). Elsevier.
- Fernandez, V. (2007). Wavelet-and svm-based forecasts: An analysis of the us metal and materials manufacturing industry. *Resources Policy*, 32, 80–89.
- Gençay, R., Selçuk, F., & Whitcher, B. J. (2001). *An introduction to wavelets and other filtering methods in finance and economics*. Elsevier.
- Giacomini, R., & Rossi, B. (2010). Forecast comparisons in unstable environments. *Journal of Applied Econometrics*, 25, 595–620.
- Granger, C. W., & Joyeux, R. (1980). An introduction to long-memory time series models and fractional differencing. *Journal of Time Series Analysis*, 1, 15–29.
- Gray, S. F. (1996). Modeling the conditional distribution of interest rates as a regime-switching process. *Journal of Financial Economics*, 42, 27–62.

- Grinsted, A., Moore, J. C., & Jevrejeva, S. (2004). Application of the cross wavelet transform and wavelet coherence to geophysical time series. *Nonlinear Processes in Geophysics*, 11, 561–566.
- Haas, M., Mittnik, S., & Paolella, M. S. (2004). A new approach to Markov-switching GARCH models. *Journal of Financial Econometrics*, 2, 493–530.
- Hamilton, J. D. (2018). Why you should never use the Hodrick–Prescott filter. *The Review of Economics and Statistics*, 100, 831–843.
- He, J., Gong, X., & Huang, L. (2021). Wavelet-temporal neural network for multivariate time series prediction. In *2021 international joint conference on neural networks* (pp. 1–8). IEEE.
- He, K., Lai, K. K., & Yen, J. (2012). Ensemble forecasting of value at risk via multi resolution analysis based methodology in metals markets. *Expert Systems with Applications*, 39, 4258–4267.
- Hodrick, R. J., & Prescott, E. C. (1997). Postwar US business cycles: An empirical investigation. *Journal of Money, Credit, and Banking*, 1–16.
- Hyndman, R. J., & Athanasopoulos, G. (2018). *Forecasting: principles and practice*. OTexts.
- Hyndman, R. J., & Khandakar, Y. (2008). Automatic time series forecasting: The forecast package for R. *Journal of Statistical Software*, 27, 1–22.
- Jin, J., & Kim, J. (2015). Forecasting natural gas prices using wavelets, time series, and artificial neural networks. *PLoS One*, 10, Article e0142064.
- John, J., Singh, S., & Kapur, M. (2020). *Inflation forecast combinations: the Indian experience*. Reserve Bank of India, Department of Economic and Policy Research.
- Jones, P. M., & Olson, E. (2013). The time-varying correlation between uncertainty, output, and inflation: Evidence from a DCC-GARCH model. *Economics Letters*, 118, 33–37.
- Jones, A. T., & Sackley, W. H. (2016). An uncertain suggestion for gold-pricing models: The effect of economic policy uncertainty on gold prices. *Journal of Economics and Finance*, 40, 367–379.
- Juntila, J., & Vataja, J. (2018). Economic policy uncertainty effects for forecasting future real economic activity. *Economic Systems*, 42, 569–583.
- Kenny, G., & Morgan, J. B. (2011). Some lessons from the financial crisis for the economic analysis. *ECB Occasional Paper no. 130*.
- Kim, S., & In, F. (2005). The relationship between stock returns and inflation: New evidence from wavelet analysis. *Journal of Empirical Finance*, 12, 435–444.
- Koning, A. J., Franses, P. H., Hibon, M., & Stekler, H. O. (2005). The M3 competition: Statistical tests of the results. *International Journal of Forecasting*, 21, 397–409.
- Leduc, S., & Liu, Z. (2016). Uncertainty shocks are aggregate demand shocks. *Journal of Monetary Economics*, 82, 20–35.
- Li, J., & Chen, W. (2014). Forecasting macroeconomic time series: Lasso-based approaches and their forecast combinations with dynamic factor models. *International Journal of Forecasting*, 30, 996–1015.
- Li, P., Hua, P., Gui, D., Niu, J., Pei, P., Zhang, J., et al. (2020). A comparative analysis of artificial neural networks and wavelet hybrid approaches to long-term toxic heavy metal prediction. *Scientific Reports*, 10, 1–15.
- Lim, B., Arik, S. Ö., Loeff, N., & Pfister, T. (2021). Temporal fusion transformers for interpretable multi-horizon time series forecasting. *International Journal of Forecasting*, 37, 1748–1764.
- Liu, L., & Zhang, T. (2015). Economic policy uncertainty and stock market volatility. *Finance Research Letters*, 15, 99–105.
- McAdam, P., & McNelis, P. (2005). Forecasting inflation with thick models and neural networks. *Economic Modelling*, 22, 848–867.
- Medeiros, M. C., Vasconcelos, G. F., Veiga, Á., & Zilberman, E. (2021). Forecasting inflation in a data-rich environment: The benefits of machine learning methods. *Journal of Business & Economic Statistics*, 39, 98–119.
- Mullainathan, S., & Spiess, J. (2017). Machine learning: An applied econometric approach. *Journal of Economic Perspectives*, 31, 87–106.
- Nakamura, E. (2005). Inflation forecasting using a neural network. *Economics Letters*, 86, 373–378.
- Nasir, M. A. (2020). Forecasting inflation under uncertainty: The forgotten dog and the frisbee. *Technological Forecasting and Social Change*, 158, Article 120172.
- Oreshkin, B. N., Carpow, D., Chapados, N., & Bengio, Y. (2019). N-beats: Neural basis expansion analysis for interpretable time series forecasting. arXiv preprint [arXiv:1905.10437](https://arxiv.org/abs/1905.10437).
- Özgür, Ö., & Akkoç, U. (2021). Inflation forecasting in an emerging economy: Selecting variables with machine learning algorithms. *International Journal of Emerging Markets*, 17, 1889–1908.
- Panja, M., Chakraborty, T., Kumar, U., & Liu, N. (2023). Epicasting: An ensemble wavelet neural network for forecasting epidemics. *Neural Networks*, 165, 185–212.
- Panja, M., Chakraborty, T., Nadim, S. S., Ghosh, I., Kumar, U., & Liu, N. (2023). An ensemble neural network approach to forecast dengue outbreak based on climatic condition. *Chaos, Solitons & Fractals*, 167, Article 113124.
- Pavlov, E. (2020). Forecasting inflation in Russia using neural networks. *Russian Journal of Money and Finance*, 79, 57–73.
- Pearson, K. (1905). The problem of the random walk. *Nature*, 72, 294.
- Percival, D. B., & Guttorp, P. (1994). Long-memory processes, the Allan variance and wavelets. vol. 4, In *Wavelet analysis and its applications* (pp. 325–344). Elsevier.
- Percival, D. B., & Mofjeld, H. O. (1997). Analysis of subtidal coastal sea level fluctuations using wavelets. *Journal of the American Statistical Association*, 92, 868–880.
- Percival, D. B., & Walden, A. T. (2000). *Wavelet methods for time series analysis volume 4*. Cambridge University Press.
- Pesaran, M. H., Shin, Y., et al. (1995). *An autoregressive distributed lag modelling approach to cointegration analysis volume 9514*. Department of Applied Economics, University of Cambridge Cambridge, UK.
- Pesquet, J.-C., Krim, H., & Carfantan, H. (1996). Time-invariant orthonormal wavelet representations. *IEEE Transactions on Signal Processing*, 44, 1964–1970.
- Phillips, P. C., & Shi, Z. (2019). Boosting the hodrick–prescott filter. *Cowles foundation discussion paper*.
- Pierce, D. A., & Haugh, L. D. (1977). Causality in temporal systems: Characterization and a survey. *Journal of Econometrics*, 5, 265–293.
- Ploberger, W., & Krämer, W. (1992). The CUSUM test with OLS residuals. *Econometrica*, 271–285.
- Pratap, B., & Sengupta, S. (2019). Macroeconomic forecasting in India: Does machine learning hold the key to better forecasts?. *RBI working paper series no. 04*.
- Pringpong, S., Maneenop, S., & Jaroenjitkam, A. (2023). Geopolitical risk and firm value: Evidence from emerging markets. *The North American Journal of Economics and Finance*, 68, Article 101951.
- Ravn, M. O., & Uhlig, H. (2002). On adjusting the Hodrick–Prescott filter for the frequency of observations. *The Review of Economics and Statistics*, 84, 371–376.
- Rossi, B., & Sekhposyan, T. (2016). Forecast rationality tests in the presence of instabilities, with applications to federal reserve and survey forecasts. *Journal of Applied Econometrics*, 31, 507–532.
- Rua, A. (2017). A wavelet-based multivariate multiscale approach for forecasting. *International Journal of Forecasting*, 33, 581–590.
- Rua, A., & Nunes, L. C. (2012). A wavelet-based assessment of market risk: The emerging markets case. *The Quarterly Review of Economics and Finance*, 52, 84–92.
- Rumelhart, D. E., Hinton, G. E., & Williams, R. J. (1986). Learning representations by back-propagating errors. *Nature*, 323, 533–536.
- Salinas, D., Flunkert, V., Gasthaus, J., & Januschowski, T. (2020). DeepAR: Probabilistic forecasting with autoregressive recurrent networks. *International Journal of Forecasting*, 36, 1181–1191.
- Salisu, A. A., Demirer, R., & Gupta, R. (2023). Policy uncertainty and stock market volatility revisited: The predictive role of signal quality. *Journal of Forecasting*, 42, 2307–2321.
- Sasal, L., Chakraborty, T., & Hadid, A. (2022). W-transformers: A wavelet-based transformer framework for univariate time series forecasting. In *2022 21st IEEE international conference on machine learning and applications* (pp. 671–676). IEEE.
- Shrestha, K., & Tan, K. H. (2005). Real interest rate parity: Long-run and short-run analysis using wavelets. *Review of Quantitative Finance and Accounting*, 25, 139–157.
- Smalter Hall, A., & Cook, T. R. (2017). Macroeconomic indicator forecasting with deep neural networks. *Federal reserve bank of Kansas City working paper*, (pp. 17–11).
- Soltani, S. (2002). On the use of the wavelet decomposition for time series prediction. *Neurocomputing*, 48, 267–277.
- Souroupanis, I., & Vivian, A. (2023). Forecasting realized volatility with wavelet decomposition. *Journal of Empirical Finance*, 74, Article 101432.

- Stock, J. H., & Watson, M. W. (2007). Why has US inflation become harder to forecast? *Journal of Money, Credit and Banking*, 39, 3–33.
- Tan, Z., Zhang, J., Wang, J., & Xu, J. (2010). Day-ahead electricity price forecasting using wavelet transform combined with arima and garch models. *Applied Energy*, 87, 3606–3610.
- Vogl, M., Rötzel, P. G., & Homes, S. (2022). Forecasting performance of wavelet neural networks and other neural network topologies: A comparative study based on financial market data sets. *Machine Learning with Applications*, 8, Article 100302.
- Vovk, V., Gammerman, A., & Shafer, G. (2005). *Algorithmic learning in a random world volume 29*. Springer.
- Walden, A. T. (2001). Wavelet analysis of discrete time series. In *European congress of mathematics* (pp. 627–641). Springer.
- Weisberg, S., & Cook, R. D. (1982). *Residuals and influence in regression*. Chapman & Hall.
- Yang, Y., & Wang, J. (2021). Forecasting wavelet neural hybrid network with financial ensemble empirical mode decomposition and mcid evaluation. *Expert Systems with Applications*, 166, Article 114097.
- Yousefi, S., Weinreich, I., & Reinartz, D. (2005). Wavelet-based prediction of oil prices. *Chaos, Solitons & Fractals*, 25, 265–275.
- Zhang, B.-L., Coggins, R., Jabri, M. A., Dersch, D., & Flower, B. (2001). Multiresolution forecasting for futures trading using wavelet decompositions. *IEEE Transactions on Neural Networks*, 12, 765–775.
- Zhang, B.-L., & Dong, Z.-Y. (2001). An adaptive neural-wavelet model for short term load forecasting. *Electric Power Systems Research*, 59, 121–129.
- Zhu, L., Wang, Y., & Fan, Q. (2014). MODWT-ARMA model for time series prediction. *Applied Mathematical Modelling*, 38, 1859–1865.